The Pennsylvania State University

The Graduate School

Department of Chemistry

ULTRAFAST DYNAMICS OF SOLVATION AND ISOTOPE EFFECTS IN DISSOCIATIVE PROCESSES

A Thesis in

Chemistry

by

Darren P. Hydutsky

Submitted in Partial Fulfillment

of the Requirements

for the Degree of

Doctor of Philosophy

May 2007

The thesis of Darren P. Hydutsky has been reviewed and approved* by the following:

A. Welford Castleman, Jr.
Eberly Distinguished Chair in Science
Evan Pugh Professor of Chemistry and Physics
Thesis Advisor
Chair of Committee

James B. Anderson
Evan Pugh Professor of Chemistry and Physics

Karl T. Mueller
Associate Professor of Chemistry

Dennis Lamb
Professor of Meteorology

Ayusman Sen
Professor of Chemistry
Head of Department of Chemistry

*Signatures are on file in the Graduate School.

ABSTRACT

The work presented here is part of an ongoing effort in the Castleman group to use clusters as a highly controllable models of phenomena in condensed phase materials. Specifically, how the properties of materials change during the progression from single molecules and atoms to bulk materials. Our focus in this work is the dynamics of atmospherically relevant species such as hydrogen iodide (HI) and sulfur dioxide (SO_2.) Specific details are presented in the Chapters 3 and 4 for the HI systems along with Chapters 5 and 6 for SO_2.

The work on HI pertains to fundamental questions on solvation, such as how many water molecules are required to form ion-pairs in the ground-state and the dynamic behavior of electronically excited species of $HI(H_2O)_n$. Additionally, $HI(H_2O)_n$ clusters serve as good models for heterogeneous processes in the atmosphere. The low coordination and high surface area of a cluster is similar to air/water and air/solid interfaces that are prevalent in aerosols. The $HI(H_2O)_n$ studies presented in this work discuss evidence for a theoretically predicted excited-state species, the biradical.

The work on SO_2 pertains to the mechanism and isotope effects in the photochemical dissociation of SO_2 at 200 to 197 nm. The motivation stems from questions regarding when the Earth's atmosphere became oxygen rich. As discussed later, isotopic anomalies in sulfur isotopes found in the Earth's rock record have been proposed as evidence of a photochemical pathway in the early atmosphere that was shut off when oxygen reached high enough levels to form an ozone layer. The work on SO_2 photochemical dissociation attempts to uncover isotope effects that would validate the

hypothesis of a photochemical mechanism being responsible for the isotope signature found in Earth's rock record.

TABLE OF CONTENTS

LIST OF FIGURES

LIST OF TABLES

ACKNOWLEDGEMENTS

I would like to thank all of the people that made this work possible. Firstly, I would like to thank my thesis advisor, A. W. Castleman, Jr., for his time, encouragement, and helpful conversations. His extensive knowledge of the field and love of science has been a great benefit and inspiration for me during these years. My thesis committee, consisting of Drs. Anderson, Jones, Lamb, and Mueller, provided constructive feedback throughout the course of my graduate work. Also, the other graduate students in the Castleman group, both past and present, have given freely of their time and energy to help me complete my thesis work. Specifically I would like to mention Sean M. Hurley for instruction and encouragement when I first arrived. Nicholas J. Bianco was very helpful in the acquisition of much of the work presented in this thesis. Of particular note, I would like to thank Troy E. Dermota for instruction and encouragement over the years. Troy always set a great example for me to follow and I am very grateful to have had him as a mentor. I would also like to thank Denis Bergeron, Ken Knappenberger, Justin Golightly, Grant Johnson and Patrick Roach for encouragement and helpful conversations. I can only hope that I have given back some small measure of what I have received.

I would also like to thank my mother, Margaret Stoeri. As my first teacher she instructed me in all the skills I would ever need and believed in me when others had given up. Finally, I would like to thank my wife, Bianca W. Hydutsky, and daughter, Ella S. Hydutsky. Bianca has been a huge support both professionally and personally,

and I will forever be in her debt. I could not have finished this work without Bianca and Ella to care for me and motivate me to succeed.

Chapter 1

Introduction

1.1 General Comments

All the work in this thesis is motivated in some manner by atmospheric chemistry. The work on $HI(H_2O)_n$ clusters aims to answer fundamental questions in current day heterogeneous atmospheric chemistry while the work on SO_2 pertains to questions about the atmosphere of the Earth billions of years ago.[1] The work performed on SO_2 monomer seeks to understand if isotopic sulfur signatures found in the Earth's rock record could have originated from photochemical processes. If the isotopic sulfur signature in the rock record can be explained by photochemical routes, then this would likely indicate the beginning of an oxygen rich atmosphere. The $HI(H_2O)_n$ experiments are concerned with the formation of ion-pairs in simple acids, both in the ground- and excited-states. Additionally, the studies on $HI(H_2O)_n$ are relevant to the physical shape of the hydrated electron.[2-6] These two systems, $HI(H_2O)_n$ and SO_2, make up the two main thrusts of this work. The remainder of the introduction presents background information for the two systems.

1.2 Background for $HI(H_2O)_n$ Studies

Heterogeneous atmospheric chemistry is of great importance to the understanding and predictions of the Earth's climate.[7] The great efforts made to understand the homogeneous chemistry of the atmosphere are the basis of our knowledge,[8] while much work remains in heterogeneous atmospheric chemistry. The multiple-phase nature of heterogeneous processes can make studying them difficult, as the chemistry of interest occurs at the interface of two phases. Clusters offer an interesting model system, as a cluster is a small amount of matter between the gas and condensed phases. Thus, we can use clusters to model small aerosol particles or ultrafine particles in the laboratory, giving us control over their size and composition.

Through interplay of homogeneous and heterogeneous methods as well as field studies,[9] it has been determined that halogens from sea-salt aerosols are one of the primary regulators of the marine boundary layers' oxidative capacity.[10, 11] Therefore, the process of halogen removal from sea-salt aerosols is of great importance. Current mechanisms require that the anions of the halogens are present in order for halogens to be removed from the aerosol (see Figure 1.1).[12] As a result, enough water must be present to dissociate the salts into their ionic components. Although not the exact system that occurs in the atmosphere, these simple acids can be introduced easily into the gas phase, and are thus more amenable to study. It is our hope that these studies will serve as a bench mark not only for sea-salt aerosols, and aid theoretical endeavors that model ions in solution.

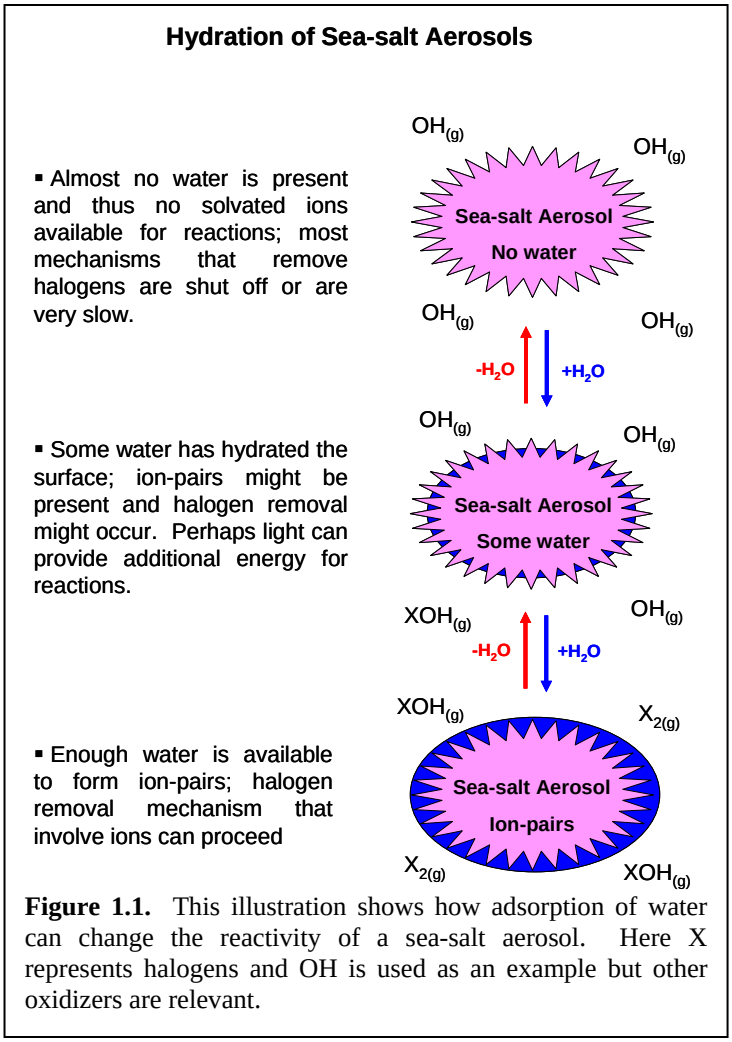

Figure 1.1. This illustration shows how adsorption of water can change the reactivity of a sea-salt aerosol. Here X represents halogens and OH is used as an example but other oxidizers are relevant.

The $HI(H_2O)_n$ system is closely related to phenomena associated with sea-salt aerosols and our previous investigations of $HX(H_2O)_n$ clusters[13-15] have sought to determine the number of water molecules required to form ion-pairs in the ground-state. For HBr, we concluded that five water molecules are needed to form ion-pairs in the ground-state,[15] while no clear threshold of ground-state ion-pair formation was observed in HI. Evidence for the ground-state ion-pair formation of HI, as well as evidence for a new kind of excited-state ionic species, known as the biradical, is presented in Chapters 3 and 4 respectively

1.3 Background for SO_2 Studies

The onset of an oxygen rich atmosphere signals an overwhelming abundance of organisms that are producing oxygen, as molecular O_2 is highly reactive and would react away unless continuously renewed. The question then is when did the Earth's atmosphere become oxygen rich as we know it today? One hypothesis[16] sites the

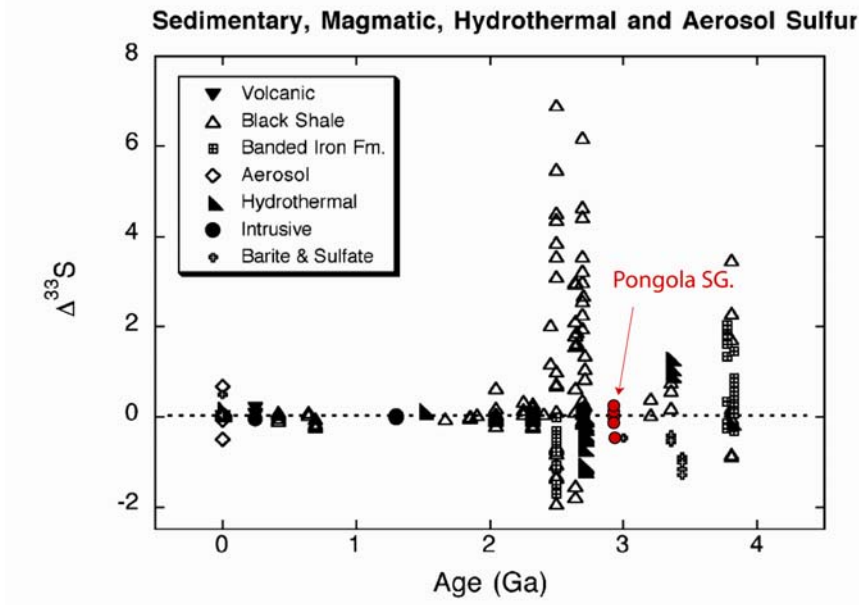

Figure 1.2. The variation in the isotopic abundance of sulfur for various samples of rock with respect to the age in billions of years. The large fluctuations are hypothesized to be the result of photochemical reaction before the onset of an oxygen rich atmosphere. Adapted and added to by S. Ono from reference 17.

variation in the isotope rock record of sulfur[17] (Figure 1.2) as evidence for the onset of an oxygen rich atmosphere.

The notation used in Figure 1.2 denotes deviation from the natural abundances of sulfur with respect to the four stable isotopes:[18]

$$\delta^{33}S = (({}^{33}S/{}^{32}S)_{sample}/({}^{33}S/{}^{32}S)_{ref} - 1)*1000 \qquad \textbf{Equation 1.1}$$

$$\delta^{34}S = (({}^{34}S/{}^{32}S)_{sample}/({}^{34}S/{}^{32}S)_{ref} - 1)*1000 \qquad \textbf{Equation 1.2}$$

$$\Delta^{33}S = \delta^{33}S - 1000*((1 + \delta^{34}S/1000)^{0.515} - 1) \qquad \textbf{Equation 1.3}$$

These variations are termed mass independent fractionation, as they deviate from normal terrestrial abundances, termed mass dependent fractionation.

Others,[19] use the sulfur signature as evidence for a thermal process caused by the unique chemical makeup of Archean life. The photochemical hypothesis assumes the absence of significant amounts of molecular oxygen, thus no ozone layer. The atmosphere would be reducing as opposed to oxidizing, as in today's atmosphere. Photochemical reactions that are not possible in today's atmosphere converted large amounts of SO_2 gas into sulfur aerosol particles (Figure 1.3) that were eventually deposited in the Earths crust. The series of reactions that formed these aerosols must have large mass-independent and mass-dependent effects in order to leave behind the large variations seen in the rock record. Other experiments have been performed[18] on the photolysis of SO_2, but the information gained from these experiments represents the compilation of all the photochemical reactions, and not the individual steps.

As a test of whether or not photochemical reactions could produce these types of isotope effects, pump-probe experiments on the dissociation of SO_2 excited by 200 to 197 nm of light were performed. Our goal was to establish if there were any isotope effects at all and to give credible physical explanations as to how these effects could occur. The details of these endeavors are presented in Chapters 5 and 6.

Chapter 5 discusses our findings in terms of the mechanistic information on how SO_2 dissociates when excited at these energies. As many before us have examined this molecule, we also compare our results with the previous work to aid in our interpretation

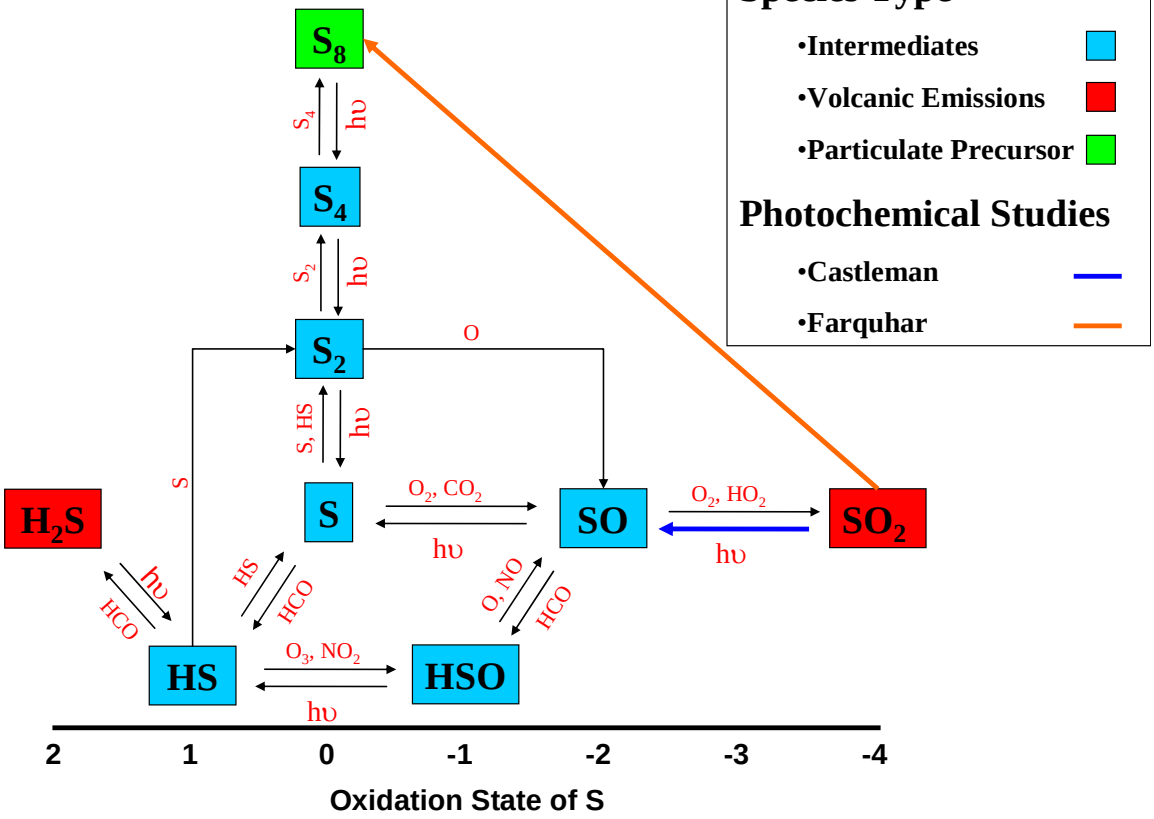

Figure 1.3. The proposed hypothesis of how photochemical reactions could produce sulfur particles that preserve isotopic variations. The colored arrows indicated the experimental work that has been done to date. Adapted from reference 16.

and to formulate a more complete picture of the dissociative event. Chapter 6 discusses the isotope effects that we observed and the physical explanation of why they are occurring. We also comment on how our results fit into the existing work regarding the onset of an oxygen rich atmosphere.

Chapter 7 presents the implications of this work, specifically what our findings mean for the theories relating to the rise of atmospheric oxygen, and what the existence of the biradical means for theories on the solvated electron. Future studies are also mentioned with specific attention to the biradical in atmospheric processes, and other experiments that could improve upon the SO_2 isotope studies performed in this work.

1.4 References

1. Pavlov, A. A.; Kasting, J. F., Mass-independent fractionation of sulfur isotopes in Archean sediments: Strong evidence for an anoxic Archean atmosphere. *Astrobiology* **2002,** 2, (1), 27-41.
2. Verlet, J. R. R.; Bragg, A. E.; Kammrath, A.; Cheshnovsky, O.; Neumark, D. M., Observation of large water-cluster anions with surface-bound excess electrons. *Science* **2005,** 307, (5706), 93-96.
3. Bragg, A. E.; Verlet, J. R. R.; Kammrath, A.; Cheshnovsky, O.; Neumark, D. M., Hydrated electron dynamics: From clusters to bulk. *Science* **2004,** 306, (5696), 669-671.
4. Headrick, J. M.; Diken, E. G.; Walters, R. S.; Hammer, N. I.; Christie, R. A.; Cui, J.; Myshakin, E. M.; Duncan, M. A.; Johnson, M. A.; Jordan, K. D., Spectral signatures of hydrated proton vibrations in water clusters. *Science* **2005,** 308, (5729), 1765-1769.
5. Hammer, N. I.; Shin, J. W.; Headrick, J. M.; Diken, E. G.; Roscioli, J. R.; Weddle, G. H.; Johnson, M. A., How do small water clusters bind an excess electron? *Science* **2004,** 306, (5696), 675-679.
6. Turi, L.; Sheu, W. S.; Rossky, P. J., Characterization of excess electrons in water-cluster anions by quantum simulations. *Science* **2005,** 309, (5736), 914-917.
7. Ramanathan, V.; Crutzen, P. J.; Kiehl, J. T.; Rosenfeld, D., Atmosphere - Aerosols, climate, and the hydrological cycle. *Science* **2001,** 294, (5549), 2119-2124.
8. Finlayson-Pitts, B. J., *Chemistry of the Upper and Lower Atmosphere*. Academic Press: San Diego, 2000.
9. Oum, K. W.; Lakin, M. J.; DeHaan, D. O.; Brauers, T.; Finlayson-Pitts, B. J., Formation of molecular chlorine from the photolysis of ozone and aqueous sea-salt particles. *Science* **1998,** 279, (5347), 74-77.
10. Platt, U., Reactive halogen species in the mid-latitude troposphere - Recent discoveries. *Water Air And Soil Pollution* **2000,** 123, (1-4), 229-244.
11. Santschi, C.; Rossi, M. J., Heterogeneous interaction of Br_2, Cl_2 and Cl_2O with solid KBr and NaCl substrates: The role of adsorbed H_2O and halogens. *Physical Chemistry Chemical Physics* **2004,** 6, (13), 3447-3460.
12. Knipping, E. M.; Lakin, M. J.; Foster, K. L.; Jungwirth, P.; Tobias, D. J.; Gerber, R. B.; Dabdub, D.; Finlayson-Pitts, B. J., Experiments and simulations of ion-enhanced interfacial chemistry on aqueous NaCl aerosols. *Science* **2000,** 288, (5464), 301-306.
13. Dermota, T. E.; Hydutsky, D. P.; Bianco, N. J.; Castleman, A. W., Photoinduced ion-pair formation in the $(HI)_m(H_2O)_n$ cluster system. *Journal Of Chemical Physics* **2005,** 123, (21).
14. Hurley, S. M.; Dermota, T. E.; Hydutsky, D. P.; Castleman, A. W., The ultrafast dynamics of HBr-water clusters: Influences on ion-pair formation. *Journal Of Chemical Physics* **2003,** 118, (20), 9272-9277.
15. Hurley, S. M.; Dermota, T. E.; Hydutsky, D. P.; Castleman, A. W., Dynamics of hydrogen bromide dissolution in the ground and excited states. *Science* **2002,** 298, (5591), 202-204.

16. Kasting, J. F., Earth history - The rise of atmospheric oxygen. *Science* **2001,** 293, (5531), 819-820.
17. Farquhar, J.; Wing, B. A., Multiple sulfur isotopes and the evolution of the atmosphere. *Earth And Planetary Science Letters* **2003,** 213, (1-2), 1-13.
18. Farquhar, J.; Savarino, J.; Airieau, S.; Thiemens, M. H., Observation of wavelength-sensitive mass-independent sulfur isotope effects during SO_2 photolysis: Implications for the early atmosphere. *Journal Of Geophysical Research-Planets* **2001,** 106, (E12), 32829-32839.
19. Ohmoto, H.; Watanabe, Y.; Ikemi, H.; Poulson, S. R.; Taylor, B. E., Sulphur isotope evidence for an oxic Archaean atmosphere. *Nature* **2006,** 442, (7105), 908-911.

Chapter 2

Experimental Methods

2.1 Experimental Techniques

The advent of pulsed femtosecond light made measuring photochemical processes on an ultra fast time scale possible. All of the experiments performed in this work made use of the pump-probe technique[1, 2] to track photochemical reactions on a sub picoseconds timescale. Thus, the initial steps of basic chemical processes can be investigated to refine our understanding. As dissociative events are often prompt (often less than 1 picosecond), the pump-probe technique is a logical choice for the SO_2 experiment. Solvent reorganization also occurs on a similar time frame, and thus this technique is also a good fit for the $HI(H_2O)_n$ system.

The pump-probe technique is a simple idea: initiate a photochemical reaction (pump), wait a controllable period of time, and arrest the photochemical reaction (probe). By varying the time between the pump and probe beam, the temporal behavior of the system in question can be examined. In Figure 2.1 we see a conceptual diagram of the pump-probe set-up employed in our laboratory. Experiments on the femtosecond to low nanosecond time scale can be most easily accomplished by varying the path length of the pump and probe beams. With knowledge of the speed of light, one can easily calculate and implement a delay between two pulses by varying the path length.

$$(3*10^{8}\ m/s)*(100*10^{-15}\ s) = 3*10^{-5}\ m \text{ or } 30\ \mu m, \qquad \textbf{Equation 2.1}$$

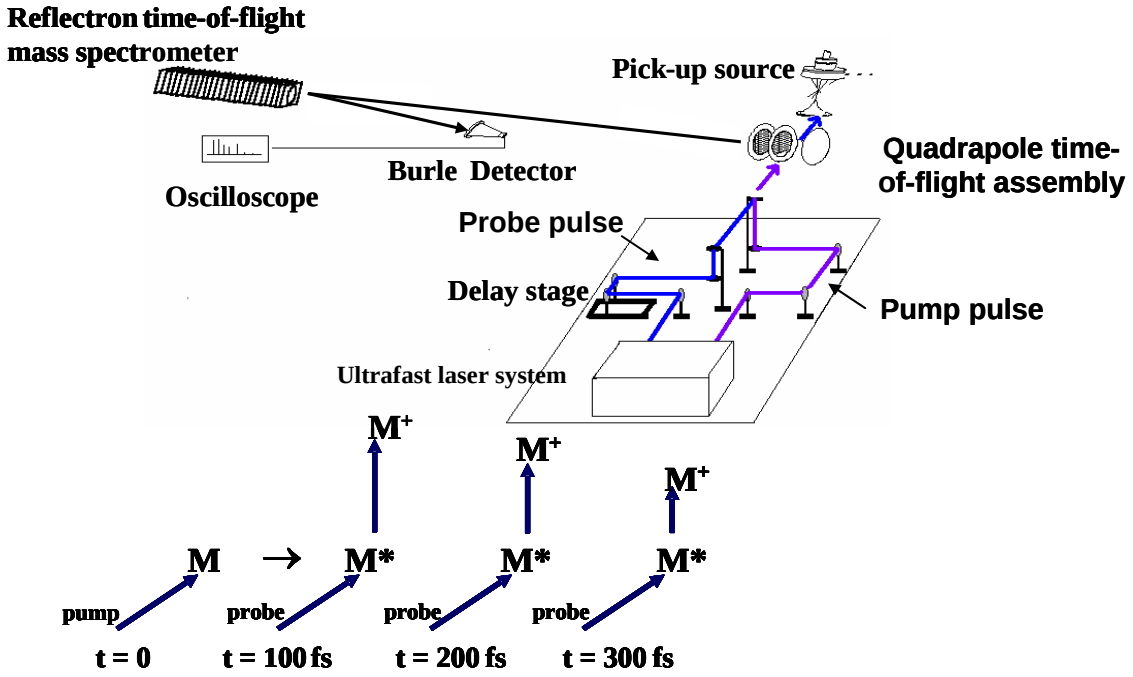

Figure 2.1. The pump and probe beam interface with the sample and detection regions of the time-of-flight mass spectrometry system. Varying the path length difference of the pump and probe beams allows us to track the change in population and absorption cross section of the clusters and molecules that we study.

Thus, a 100 femtosecond delay is equivalent to a path length that is 30 μm in length. Longer time frames are more suited to varying the time electronically as the distance needed to change the arrival time by many nanoseconds requires large movable stages (one nanosecond requires a path length change of 0.3 m).

Detection is achieved by laser ionization followed by time-of-flight mass spectrometry. The small size of the sample makes other detection methods, such as absorption or florescence, more difficult to perform. The time-of-flight assembly and reflectron were constructed previously, and are based on the designs of Martin et. al.[3, 4] Ionization and mass spectrometry also provides the added benefit of distinctly identifying all the species involved, though fragmentation is always an issue. For example, the species detected in the $HI(H_2O)_n$ system for the $HI(H_2O)$ cluster is H_3O^+, because the

internal energy released by the reorganization around the ion is higher than the binding energy of the iodine atom. In the SO_2 system, ion-state fragmentation caused complications in the analysis of the SO product. In general, these shortcomings can be overcome and specific instances are addressed in later Chapters.

Ion-state fragmentation deserves some further explanation, as this process often occurs during power studies with the probe laser, which is discussed later. Often the chromophore of an experiment absorbs more photons than are necessary to ionize the molecule or cluster. When this occurs, the chromophore involved could fragment depending on the nature of the cationic potential energy surface. As this process occurs at the same time as the ionization, two masses of the same origin are detected. Confirmation of ion-state fragmentation in a pump-probe experiment is very easy because the transients of the intact and ion-state fragmentation product are nearly identical since they come from the same neutral precursor. Normally, ion-state fragmentation is a minor inconvenience, resulting only in a more congested mass spectrum. However, if a neutral-state dissociation is also occurring in the same experiment, ion-state fragmentation will overlap with the neutral-state dissociation obscuring the neutral-state dynamics of the dissociation product. The details of how one can get around this are discussed further in Chapter 5.

Power studies are used to determine the number of photons that a specific molecule or cluster absorbed to ionize. Power studies can also be used to deconvolute a system where the pump beam excites two different electronic states.[5-7] All of the experiments discussed in this thesis are one-photon excitations, as two photons of the pump ionize SO_2 and HI. In the SO_2 experiments, power studies are used to examine the

subtle effects that the isotopes of sulfur have on the ionization process in our experiment. In the HI system, power studies are used to determine whether the I atom is closely associated with the cluster or not. Performing power studies requires that all conditions remain stable except for the probe power. The requirement of stability may sound obvious but is of critical importance in these experiments because of our detection scheme. Our experiments measure relative intensities for all of the ions in the spectrum, so changes in molecular beam position and laser power will affect the intensity of the species. The ion signal follows the following equation:

$$I = P^{\lambda}, \qquad \textbf{Equation 2.2}$$

where P is the power of the probe pulse, I is the signal intensity of the molecule or cluster of interest, and λ is the number of photons required for the signal to appear or, in our case, to be ionize the species being interrogated. Thus, if the natural log of I and P are plotted, a linear regression can be used to solve for the slope of the line, λ. In some of the power studies performed λ values were obtained that made no physical sense. The strange λ values were tracked back to the low total power of our laser (2^{nd} harmonic total power at the Brewster's window is 2 mW) and the thermal noise in the room. Since molecules or atoms of known ionization potential are present in our experiment and our data is precise (R^2 values of the linear regression are close to 1), we can use these molecules or atoms to internally calibrate the power study. For example, the I atom has a known ionization potential of 10.45 eV, then photons with 3.1 eV of energy ionizes the I atom with a four photon absorption. Thus if our power study returns a value of five

photons we adjust the power of each reading by the same amount to calibrate the power study to the known power dependence of the I atom, namely four photons.

2.2 References

1. Rosker, M. J.; Dantus, M.; Zewail, A. H., Femtosecond Clocking Of The Chemical-Bond. *Science* **1988,** 241, (4870), 1200-1202.
2. Zewail, A. H., Laser Femtochemistry. *Science* **1988,** 242, (4886), 1645-1653.
3. Bergmann, T.; Martin, T. P.; Schaber, H., High-Resolution Time-Of-Flight Mass Spectrometers.2. Reflector Design. *Review Of Scientific Instruments* **1990,** 61, (10), 2592-2600.
4. Bergmann, T.; Goehlich, H.; Martin, T. P.; Schaber, H.; Malegiannakis, G., High-Resolution Time-Of-Flight Mass Spectrometers.2. Cross Beam Ion Optics. *Review Of Scientific Instruments* **1990,** 61, (10), 2585-2591.
5. Dermota, T. E.; Hydutsky, A. P.; Bianco, N. J.; Castleman, A. W., Excited-state dynamics of $(SO_2)_m$ clusters. *Journal Of Physical Chemistry A* **2005,** 109, (37), 8259-8267.
6. Dermota, T. E.; Hydutsky, D. P.; Bianco, N. J.; Castleman, A. W., Ultrafast dynamics of the $SO_2(H_2O)_n$ cluster system. *Journal Of Physical Chemistry A* **2005,** 109, (37), 8254-8258.
7. Knappenberger, K. L.; Castleman, A. W., Photodissociation of sulfur dioxide: The E state revisited. *Journal Of Physical Chemistry A* **2004,** 108, (1), 9-14.

Chapter 3

The Solvation and Photochemistry of $HI(H_2O)_n$ Clusters: Evidence of Excited-state Biradical Formation and Implications to the Solvated Electron

3.1 Abstract

While investigating the solvation and photochemical dynamics of $HI(H_2O)_n$ clusters, we observed unusual dynamics associated with the iodine atoms. Upon further experimentation we concluded that we had experimental evidence for the theoretically predicted biradical species[1] consisting of a halo acid clustered to water molecules. Importantly, the excited biradical theory also fits experimentally observable phenomena pertaining to the hydrated electron. Hence, the observation of an excited biradical structure also has implications to physical interpretation of the hydrated electron. Our observations, combined with others, raise enough new questions to reevaluate the idea of hydrated hydronium as a possible physical moiety for the hydrated electron.

3.2 Introduction

Recent work on the hydrated electron aims at understanding, through the use of gas phase and computational methods, the amount of water necessary to capture an electron in a cavity. Binding motifs have been studied extensively, and unique structures

have come from this work,[2-4] as well as from studies of the ultrafast dynamics of the hydrated electron.[5] The exciting interplay of experiment[6-8] and theory[9] has scrutinized the results, bringing to light the fact that though large clusters of water have been studied up to $(H_2O)_{200}^-$,[10] no definitive evidence for cavity-bound electrons has been reported to date in the gas phase. This perplexing realization has come many years after the discovery of the hydrated electron[11] in bulk water. However, even in bulk systems the hydrated electron has displayed strange behavior. Recent experiments on pressure and temperature effects of the hydrated electron[12] have shown that there is only a small increase in the cavity radius of the hydrated electron, even when the density is dropped to as low as 0.1 g/mL. We present in this report experimental evidence of a gas phase species that validates alternative theories of the hydrated electron, the most recent being the biradical species reported by Domcke.[1, 13]

The biradical has ionic character[1, 13] and has been proposed as an alternative

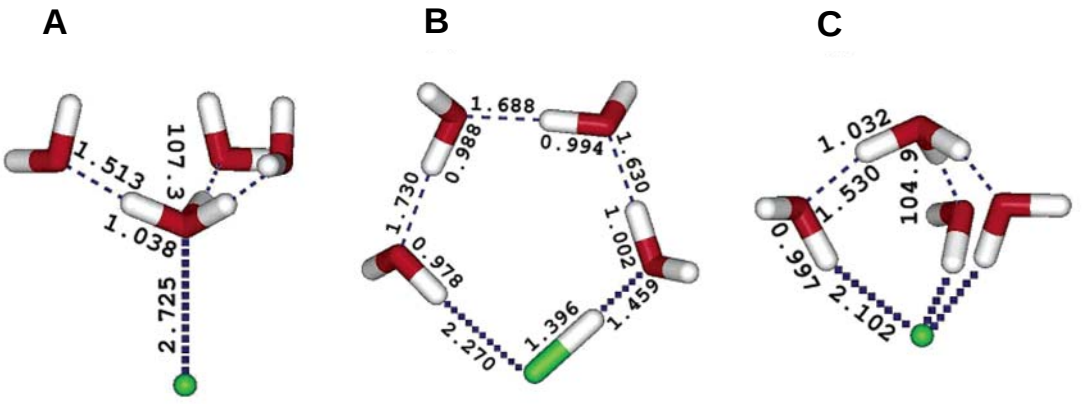

Figure 3.1. Three possible structures of the neutral species in our experiment wherein a biradical species is believed to be generated upon excitation: **A,** represents the biradical structure, **B,** represents an $HX(H_2O)_n$ where ion-pair formation of the halo acid HX has not occurred and the H-X molecule is still intact, and **C,** represents ion-pair structure. Note in the biradical structure the X has only one bond and that bound is longer (thus weaker) than in the ion-pair case where there are three shorter bonds. All bond lengths are in angstroms. Adapted from reference 14.

moiety to the electron in a cavity model known as the solvated, or hydrated electron in cases where the solvent is water. Figure 3.1 **A** shows a biradical structure for an $HX(H_2O)_4$ cluster,[14] where X is a halogen. The other structures shown are, **B,** a covalently bound species, where the H-X bond is still intact, and **C,** an ion-pair structure where the H-X bond has been broken. The biradical is an excited-state species that has been calculated for pure water,[13] methanol,[15] or a halo acid solvated by water.[14]

Though it may seem controversial, over the years others have proposed alternative structures for the hydrated electron.[16-18] These theories differ from the cavity model in that they explain the observed phenomena with a solvent-electron moiety or with hydrated hydronium, thus avoiding the need for a cavity in solution. The solvated electron is known to manifest itself in many solvents where an electron is released from a solute, or from a solvent molecule by radiation, and is captured by the surrounding solvent. Cavity models of the solvated electron contend that the electron is captured in a void space in the solvent. The model was originally proposed for ammonia with alkaline metals as the solute and was later used to describe the radiolysis of water and other solvents. The assignment of a cavity is largely due to the similarity of the solvated electron to an f-center defect (anion vacancies in solids) in terms of the hydrated electrons optical absorption and, in the case of the solvated electron of ammonia and alkaline metals, the increase in molar volume.

The solvation of halo acids are a phenomenon of long standing interest, bearing on fundamental issues of ion-pair formation, as well as ones pertaining to atmospheric science.[19] Prior studies in our laboratory of HBr[20, 21] and HI[22] by solvated water clusters have interrogated the dynamics of solvent reorganization around newly formed ion-pairs.

Further exploration of $HI(H_2O)_n$ clusters has lead to unexpected dynamics associated with the iodine atom evolving from $HI(H_2O)_n$ clusters. Below we present evidence of an excited-state species, much like the biradical, that explains our experimental results.

3.3 HI Solvation and the Biradical Species

The femtosecond pump-probe technique[23] was employed to track the dynamics of the $HI(H_2O)_n$ clusters. The technique consists of a pump pulse to start and a probe pulse to monitor photochemical reactions. Our 10 Hz laser system produces pulses centered at 800 nm, with a temporal width of 100 femtoseconds, a band width of 20 nm, and a power of 2.5 mJ/pulse. Second, third, and fourth harmonics are produced by an in-house harmonic box. Time-of–flight mass spectrometry was used to identify the clusters and atomic products arising from the photo-induced reactions following ionization by the probe beam. A mixture of 20% HI, 20% argon, and 60 % helium was made to a final pressure of 3 to 4 atm and expanded into the ionization region through a Park solenoid valve. The inside orifice of the solenoid valve was 500 μm in diameter and the outside diameter was conically expanded to ~1.75 mm for effective pick-up of water molecules. The molecular beam passes through an effusive plume of water vapor, created by a pick-up source,[24, 25] where the $(HI)_n$ clusters undergo a replacement reaction with the water vapor, forming $HI(H_2O)_n$ clusters.

During the course of our experiments on $HI(H_2O)_n$ clusters we observed a long growth in the I^+ transient (see Figure 3.2). Since the dynamics seen in the I atom could have originated from any of the species seen in the cluster distribution, we performed

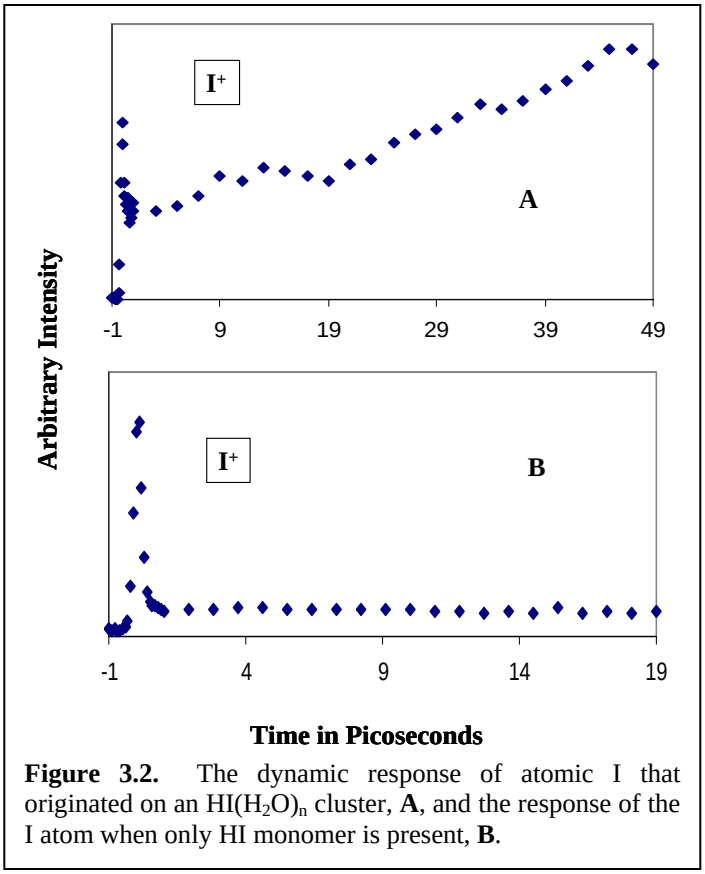

Figure 3.2. The dynamic response of atomic I that originated on an $HI(H_2O)_n$ cluster, **A**, and the response of the I atom when only HI monomer is present, **B**.

several control experiments to confirm that the dynamics seen were the result of I atoms that dissociate from an $HI(H_2O)_n$ cluster. HI monomer and HI cluster experiments were performed and only a small plateau (Figure 3.2., B) was seen in the HI monomer and a decay in the HI clusters experiments with no water. We therefore conclude that the dynamics seen in the I atom with water present originates from the $HI(H_2O)_n$ clusters.

Additionally, ionization studies of the I atom were performed under varying conditions of probe power to determine the internal energy of the I atom. As shown in Figure 3.3 the I atom that evolves off of HI monomer has the same power dependence as the I atom that evolves of the $HI(H_2O)_n$ clusters. This information combined with known ionization potential of the I atom (10.45 eV) allows us to gauge the internal energy of a cluster or atom. Our power studies reveal that the I atom from the $HI(H_2O)_n$ clusters has

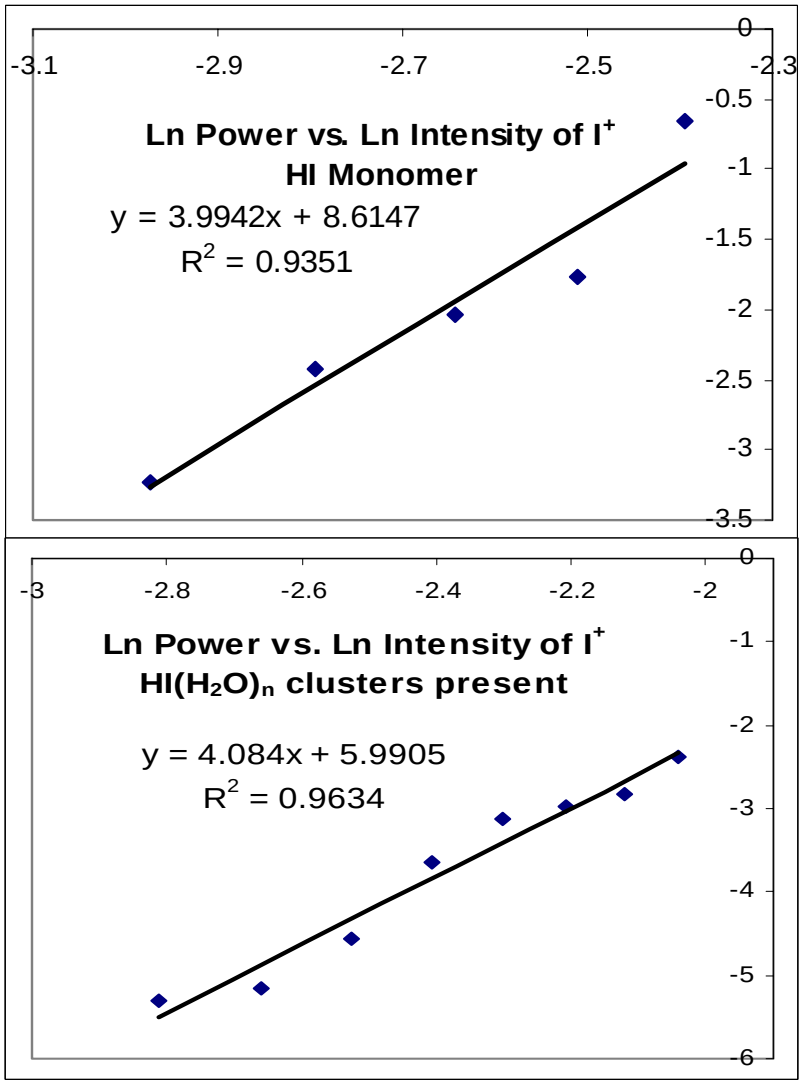

Figure 3.3. Power studies of the I atom from dissociation of HI monomer and from $HI(H_2O)_n$ clusters. The I atom from both the HI monomer and $HI(H_2O)_n$ clusters have the same photon dependence.

the same power dependence as the I atoms that dissociate from HI monomer and thus are either in the ground or first spin-excited state of the I atom.[26] The HI monomer is well known to predissociate when excited at these energies,[27] and thus the potential influence of caging[28, 29] needs to be considered. Caging is a process where a chromophore that is dissociative at a given excitation energy is clustered with solvent molecules that physically block the atom from dissociating. At first glance a caging mechanism would appear to fit our data. If caging is occurring we would expect to observe I atoms

dissociating from the smallest $HI(H_2O)_n$ clusters. Thus, a likely product of this I atom dissociation would be a H_3O radical. The ionization potential of D_3O is known (4.3 eV) and we can assume that the ionization potential of H_3O is similar. Given the pump energy (6.2 eV), the dissociation energy of HI (3.20 eV, though solvation will decrease this number), and the maximum internal energy of the I atom (0.94 eV), we can approximate the energy needed to ionize an H_3O that resulted form a $HI(H_2O)$ cluster that dissociated an I atom.

$HI(H_2O) + \lambda_{pump} \rightarrow HI(H_2O)^*$	6.2 eV
$HI(H_2O)^* \rightarrow H_3O + I$	~ -3.20eV
$H_3O \rightarrow H_3O^+$	-4.3 eV
$I \rightarrow I^*$	-0.94 eV
_____	
$HI(H_2O) + \lambda_{pump} \rightarrow H_3O^+ + I^*$	-2.24 eV

Given that the probe photons have an energy of 3.1 eV, an H_3O from a $HI(H_2O)$ cluster is ionized with one photon of the probe. However, power studies employed at a 75 picosecond delay (Table 3.1) revealed that the smallest $HI(H_2O)_n$ clusters do not have photon counts of one, but of four. If caging is occurring, it is not the only mechanism; as we see evidence from the 4 photon counts that the I atom is still attached to the $HI(H_2O)$ cluster. Also, the $HI(H_2O)_6$ clusters shows evidence of I atom dissociation from the photon count of one. In a caging dominated mechanism more solvent molecules should more effectively cage the dissociating species, thus this is the opposite solvation trend that would be expected to occur in a caging dominated mechanism.

Table 3.1

Originally Excited Species	Ion detected	Ionization Potential	E_p	Photon Count 75 ps	Photon Count Expected	Ionized Species
$HI(H_2O)$	$H^+(H_2O)$	9.45-10.39	6.2	4	2	$HI(H_2O)$
$HI(H_2O)_2$	$H^+(H_2O)_2$	9.45-10.39	6.2	3	2	$HI(H_2O)_2$
$HI(H_2O)_3$	$H^+(H_2O)_3$	9.45-10.39	6.2	2	2	$HI(H_2O)_3$
$HI(H_2O)_4$	$H^+(H_2O)_4$	9.45-10.39	6.2	2	2	$HI(H_2O)_4$
$HI(H_2O)_5$	$H^+(H_2O)_5$	9.45-10.39	6.2	2	2	$HI(H_2O)_5$
$HI(H_2O)_6$	$H^+(H_2O)_6$	9.45-10.39	6.2	1	2	$H(H_2O)_6$
-	I^+	10.45	-	4	4	I

The photon counts and ionization potentials for all the $HI(H_2O)_n$ clusters and the I atom. All energies are in eV, E_p is the energy of the pump and the probe energy is 3.1 eV.

In summary of our experimental results we have: 1) an I atom that dissociates from an $HI(H_2O)_n$ or clusters, 2) this I atom is electronically similar to an I atom from the dissociation of HI at these wavelengths of excitation, and 3) a caging mechanism does not fully account for the findings as the solvation trend is reversed.

3.4 Discussion

If the dynamics that are evident in the I atom are not exclusively from caging, we must therefore account for the behavior in terms of another event. In van der Waals bound clusters, evaporation of single molecules or atoms takes place when the internal energy in the cluster redistributes into rovibrational bonds and exceeds the binding energy of the most weakly bound molecule or atom. In the case of the $HI(H_2O)_n$ clusters that we studied, an I atom could evaporate if the species involved is a biradical like that seen in Figure 3.1, **A**. Since caging does not completely explain the trend in photon counts shown in Table 3.1, evaporation of the I atom from the $HI(H_2O)_6$ cluster becomes the likely mechanism. Evaporation of an I atom occurs in the $HI(H_2O)_6$ clusters because

this cluster will have the largest amount of internal energy from solvation. Evaporation from the $HI(H_2O)_6$ cluster suggests that the I atom is the most weakly bound species. Computational work[14] predicts just such a structure for the excited-state biradical for another hydrogen halide, consisting of an $HCl(H_2O)_4$ cluster. Since the I atom leaves the cluster through an evaporative process, and all of the clusters are long-lived, we conclude that we have experimentally observed a bound excited-state with a loosely bound I, very similar to the predicted biradical.

Table 3.1 show a marked decrease in photon counts for ionization as the number of water molecule increases. As discussed above, this trend precludes a caging dominated mechanism from our interpretation. Additionally, the trend in photon counts could be associated with ion-pair formation in the ground-state. The other clusters will be discussed in Chapter 4 as the thrust of Chapter 3 is the growth in the I atom and the evidence for the biradical.

Figure 3.4 summarizes the results of our experiments. Upon excitation by 6.2 eV of energy, the $HI(H_2O)_n$ cluster reorganizes to a structure similar to the biradical. The largest cluster seen, the $HI(H_2O)_6$, has a photon count of one and dissociates an I atom. More solvent molecules facilitate the formation of the biradical and the ensuing dissociation, thus precluding a caging mechanism and facilitating an evaporative mechanism. As an evaporative process seems likely and given the long growth for the I atom dissociation, the electronic state at 6.2 eV appears to be bound. We thus conclude that the species we are observing in our molecular beam is similar to the proposed biradical.

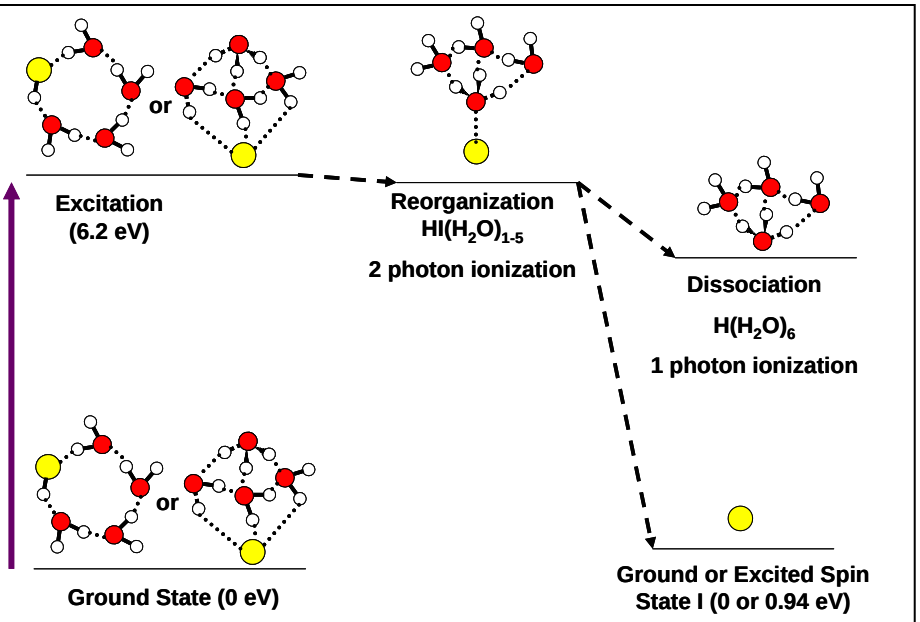

Figure 3.4. . The energetic and dynamics of a $HI(H_2O)_4$ cluster as it excited to what we believe to be a biradical like excited-state.

3.5 Conclusion

With strong evidence for the existence of a biradical-like species, a discussion of hydrated electrons in terms of a similar model is fitting. The electron in a cavity model was originally used to describe the phenomena of dissolving an alkali metal in liquid ammonia. The result is an f center-like species and an increase in molar volume. F centers are well known in solids,[30] being vacancies of anions where an electron can reside. The phenomenon that occurs in water upon radiation of the solution does produce a spectral signature similar to that seen in the ammonia case, but spectral signatures are not unquestionable evidence of physical structures. Estimates of the change in partial molar volume from pressure dependent kinetics studies predict a negative molar volume or an increase in the density of the solution,[31] while recent photoacoustic measurements place the partial molar volume of the solvated electron in water at 26 mL/mol.[32] The small increase in molar volume despite the assertion of the formation of void spaces is

rationalized in the cavity model by postulating that the hydrogen bonding network in water strengthens, thus reducing any increase in molar volume. Additionally, ion mobility studies of the hydrated electron in water[33, 34] have shown the mobility to be similar to that of an OH^- moiety. The concept of a void space propagating through a solution at the same rate as OH^- is difficult to rationalize. Given the known OH^- exchange mechanism that propagates by moving charge, but moving heavy atoms like oxygen very little, it is difficult to believe that a void space could move at a similar rate. As stated earlier, density experiments on supercritical water fit to current models that relate the spectral aspects of the hydrated electron to cavity size have shown only a small increase in cavity size when the density of the solution is decreased to 0.1 g/mL.[12] Thus, we believe that evidence of the biradical reported herein and else where,[35] and the arguments given above, support the alternative excited-state moiety process proposed by Domcke. The biradical moiety also explains the observable phenomena, but it does not require the formation of void space in solution.

In summary, we conclude the following: 1) there is a bound state in the vicinity of our 6.2 eV excitation energy for the $HI(H_2O)_n$ cluster, 2) this state evolves a ground-state or spin-excited state neutral I atom on a time scale and at an internal energy consistent with an evaporative process, 3) the present observations are consistent with a structure like the predicted biradical species of Domke.[14] We conclude from the above data and discussion that our experiments are indeed producing a biradical-like species, as predicted theoretically, and observed here experimentally. Establishing the existence of a biradical species gives credence to the alternative interpretation of the hydrated electron in water, and illustrates the potential of small-cluster systems to complement

experimentation in the bulk. Given the recent developments in other cluster works related to the solved electron, consideration of an alternative to a traditional electron in a cavity model deserves careful scrutiny. Future experiments will aim to gauge the atmospheric significance of the biradical in $NaI(H_2O)_n$ clusters, where the wavelengths needed to excite this species will be atmospherically relevant. Additionally, we might be able to use excited-state biradical formation to distinguish between ground-state ion-pair formation and covalently bound species in simple acids. If further experimental and computational work can confirm the observations of this work, these biradical species might better explain many phenomena that are currently thought to be the result of cavity-bound hydrated electrons.

3.6 References

1. Sobolewski, A. L.; Domcke, W., Hydrated hydronium: a cluster model of the solvated electron? *Physical Chemistry Chemical Physics* **2002,** 4, (1), 4-10.
2. Headrick, J. M.; Diken, E. G.; Walters, R. S.; Hammer, N. I.; Christie, R. A.; Cui, J.; Myshakin, E. M.; Duncan, M. A.; Johnson, M. A.; Jordan, K. D., Spectral signatures of hydrated proton vibrations in water clusters. *Science* **2005,** 308, (5729), 1765-1769.
3. Hammer, N. I.; Shin, J. W.; Headrick, J. M.; Diken, E. G.; Roscioli, J. R.; Weddle, G. H.; Johnson, M. A., How do small water clusters bind an excess electron? *Science* **2004,** 306, (5696), 675-679.
4. Hammer, N. I.; Roscioli, J. R.; Johnson, M. A.; Myshakin, E. M.; Jordan, K. D., Infrared spectrum and structural assignment of the water trimer anion. *Journal Of Physical Chemistry A* **2005,** 109, (50), 11526-11530.
5. Paik, D. H.; Lee, I. R.; Yang, D. S.; Baskin, J. S.; Zewail, A. H., Electrons in finite-sized water cavities: Hydration dynamics observed in real time. *Science* **2004,** 306, (5696), 672-675.
6. Verlet, J. R. R.; Bragg, A. E.; Kammrath, A.; Cheshnovsky, O.; Neumark, D. M., Comment on "Characterization of excess electrons in water-cluster anions by quantum simulations". *Science* **2005,** 310, (5755).

7. Verlet, J. R. R.; Bragg, A. E.; Kammrath, A.; Cheshnovsky, O.; Neumark, D. M., Observation of large water-cluster anions with surface-bound excess electrons. *Science* **2005,** 307, (5706), 93-96.
8. Bragg, A. E.; Verlet, J. R. R.; Kammrath, A.; Cheshnovsky, O.; Neumark, D. M., Hydrated electron dynamics: From clusters to bulk. *Science* **2004,** 306, (5696), 669-671.
9. Turi, L.; Sheu, W. S.; Rossky, P. J., Characterization of excess electrons in water-cluster anions by quantum simulations. *Science* **2005,** 309, (5736), 914-917.
10. Kammrath, A.; Verlet, J. R. R.; Griffin, G. B.; Neumark, D. M., Photoelectron spectroscopy of large $(water)_n^-$ (n=50-200) clusters at 4.7 eV. *Journal Of Chemical Physics* **2006,** 125, (7).
11. Hart, E. J.; Boag, J. W., Absorption Spectrum Of Hydrated Electron In Water And In Aqueous Solutions. *Journal Of The American Chemical Society* **1962,** 84, (21), 4090-&.
12. Bartels, D. M.; Takahashi, K.; Cline, J. A.; Marin, T. W.; Jonah, C. D., Pulse radiolysis of supercritical water. 3. Spectrum and thermodynamics of the hydrated electron. *Journal Of Physical Chemistry A* **2005,** 109, (7), 1299-1307.
13. Sobolewski, A. L.; Domcke, W., Photochemistry of water: The $(H_2O)_5$ cluster. *Journal Of Chemical Physics* **2005,** 122.
14. Sobolewski, A. L.; Domcke, W., Photochemistry of $HCl(H_2O)_4$: Cluster model of the photodetachment of the chloride anion in water. *Journal Of Physical Chemistry A* **2003,** 107, (10), 1557-1562.
15. Neumann, S.; Eisfeld, W.; Sobolewski, A. L.; Domcke, W., Resonance Raman spectrum of the solvated electron in methanol: Simulation within a cluster model. *Journal Of Physical Chemistry A* **2006,** 110, (17), 5613-5619.
16. Tuttle, T. R.; Golden, S., Resolution Of Optical-Spectra Of Solvated Electrons In Water. *Journal Of Physical Chemistry* **1980,** 84, (19), 2457-2458.
17. Hameka, H. F.; Robinson, G. W.; Marsden, C. J., Structure Of The Hydrated Electron. *Journal Of Physical Chemistry* **1987,** 91, (12), 3150-3157.
18. Muguet, F. F.; Gelabert, H.; Gauduel, Y., Electron propagator study of the excitation spectrum of the solvated hydronium radical. *Journal De Chimie Physique Et De Physico-Chimie Biologique* **1996,** 93, (10), 1808-1827.
19. Gertner, B. J.; Hynes, J. T., Molecular dynamics simulation of hydrochloric acid ionization at the surface of stratospheric ice. *Science* **1996,** 271, (5255), 1563-1566.
20. Hurley, S. M.; Dermota, T. E.; Hydutsky, D. P.; Castleman, A. W., The ultrafast dynamics of HBr-water clusters: Influences on ion-pair formation. *Journal Of Chemical Physics* **2003,** 118, (20), 9272-9277.
21. Hurley, S. M.; Dermota, T. E.; Hydutsky, D. P.; Castleman, A. W., Dynamics of hydrogen bromide dissolution in the ground and excited states. *Science* **2002,** 298, (5591), 202-204.
22. Dermota, T. E.; Hydutsky, D. P.; Bianco, N. J.; Castleman, A. W., Photoinduced ion-pair formation in the $(HI)_m(H_2O)_n$ cluster system. *Journal Of Chemical Physics* **2005,** 123.
23. Zewail, A. H., Laser Femtochemistry. *Science* **1988,** 242, (4886), 1645-1653.
24. Goyal, S.; Robinson, G. N.; Schutt, D. L.; Scoles, G., Infrared-Spectroscopy Of SF_6 In And On Argon Clusters In An Extended Range Of Cluster Sizes - Finite-Size

Particles Attaining Bulk-Like Properties. *Journal Of Physical Chemistry* **1991,** 95, (11), 4186-4189.
25. Gough, T. E.; Knight, D. G.; Scoles, G., Matrix Spectroscopy In The Gas-Phase - Ir Spectroscopy Of Argon Clusters Containing SF_6 Or CH_3F. *Chemical Physics Letters* **1983,** 97, (2), 155-160.
26. Chichinin, A. I., Chemical properties of electronically excited halogen atoms $X(^2P_{1/2})$ (X=F,Cl,Br,I). *Journal Of Physical And Chemical Reference Data* **2006,** 35, (2), 869-928.
27. Gendron, D. J.; Hepburn, J. W., Dynamics of Hl photodissociation in the A band absorption via H-atom Doppler spectroscopy. *Journal Of Chemical Physics* **1998,** 109, (17), 7205-7213.
28. Alexander, M. L.; Levinger, N. E.; Johnson, M. A.; Ray, D.; Lineberger, W. C., Recombination Of Br_2^- Photodissociated Within Mass Selected Ionic Clusters. *Journal Of Chemical Physics* **1988,** 88, (10), 6200-6210.
29. Knappenberger, K. L.; Castleman, A. W., The influence of cluster formation on the photodissociation of sulfur dioxide: Excitation to the E state. *Journal Of Chemical Physics* **2004,** 121, (8), 3540-3549.
30. Fowler, W. B., Electronic States Of F Center In Alkali Halide Crystals. *Physical Review* **1968,** 174, (3), 988.
31. Hart, E. J.; Anbar, M., *The hydrated electron*. Wiley-Interscience: New York, 1970; p 267.
32. Borsarelli, C. D., The partial molar volumes of hydrated proton and electron determined with time-resolved photoacoustic. *Journal De Physique IV* **2005,** 125, 11-13.
33. Schmidt, K. H.; Ander, S. M., Formation And Recombination Of H_3O^+ And Hydroxide In Irradiated Water. *Journal Of Physical Chemistry* **1969,** 73, (9), 2846-2852.
34. Schmidt, K. H.; Han, P.; Bartels, D. M., Temperature-Dependence Of Solvated Electron-Diffusion In H_2O And D_2O. *Journal Of Physical Chemistry* **1992,** 96, (1), 199-206.
35. Poterya, V.; Farnik, M.; Slavicek, P.; Buck, U.; Kresin, V. V., Photodissociation of hydrogen halide molecules on free ice nanoparticles. *Journal Of Chemical Physics* **2007,** 126, (7).

Chapter 4

Ion-pair Formation, Hydrated Electron, and Biradical: Dynamics Study of $HI(H_2O)_n$ Clusters at 200 nm Excitation

4.1 Abstract

Pump-probe experiments at 200 nm of excitation energy and a 400 nm probe have been performed on $HI(H_2O)_n$ cluster. Evidence supporting that three water molecules are necessary to form ground-state ion-pairs, as predicted theoretically, is presented. We present further evidence that the structure of the excited $HI(H_2O)_n$ clusters in this study is similar to the proposed biradical structure. The molecule by molecule solvation of the HI chromophore is discussed in regards to the dynamics experiments and power studies that were performed.

4.2 Introduction

Solvation of simple acids has been a long standing interest of our group.[1-3] During this time we have been successful in determining the number of water molecules necessary to form ground-state ion-pairs in $HBr(H_2O)_n$ clusters,[1] and we have examined solvent reorganization in $HBr(H_2O)_n$[4] and $HI(H_2O)_n$[2] clusters. Our motivation has come from the many processes in nature that involve solvated ions. Specifically, we would like

to understand the mechanism involved in the removal of halogens from sea-salt aerosols[5, 6] and how ion-pair formation can influence nucleation processes.[7]

We have presented experimental evidence in Chapter 3 for a theoretically predicted excited-state species, the biradical.[8] The biradical is of particular interest to us and the scientific community[9-13] because it has been proposed as an alternative moiety to the cavity model of the hydrated electron. Additionally, the biradical could be useful in explaining photochemically induced halogen loss in sea-salt aerosols. In a similar system, like $NaI(H_2O)_n$, the wavelength of light necessary to excite the biradical might be present in the atmosphere. Thus, these studies can be viewed as a groundwork to studies on $NaI(H_2O)_n$ clusters.

4.3 Experimental

The instrument used in these experiments consists of a femtosecond laser system that produces 100 fs pulses, at 10 Hz, with 2.5 mJ per pulse, centered at 800 nm. The fundamental is frequency doubled and mixed to produce second, third, and fourth harmonics. The second harmonic was used for the probe beam and the fourth harmonic was used for the pump beam in all of the pump-probe experiments presented. HI gas was made by drying concentrated HI solution (Sigma Aldrich) with P_2O_5 under vacuum.[2] A mixture of 20 % HI, 20 % argon and 60 % helium at a final pressure of 3 to 4 atm. was introduced by a Parker solenoid valve. The molecular beam passed through a effusive plume of water vapor created by a continuous flow pick-up source.[14, 15] The inside orifice of the solenoid valve was 500 μm in diameter and the outside diameter was

conically expanded to ~1.75 mm to shape the molecular beam for effective pick-up of water molecules. Detection of ionized clusters was performed with a home-built time-of-flight mass spectrometer consisting of a quadrapole time-of-flight assembly,[16] a reflection,[17] and a Burel bipolar detector. Signal from the detector was acquired by a Tektronics oscilloscope model TDS5104B.

4.4 Results

Figure 4.1 shows a representative mass spectrum of our cluster distribution. The clusters labeled $H^+(H_2O)_n$ are the result of a cluster initially of the form $HI(H_2O)_n$. Upon ionization the I atom evaporates from the cluster as it is poorly bound in the cation form and the ionization process releases internal energy after reorganization around the charge.[4] Also, I atoms can dissociate from the cluster in the neutral state after excitation by the pump beam. Power studies of the ionization process have been used to determine when the neutral cluster is intact. The same explanation holds true for the $(HI)_2(H_2O)_n$ cluster observed as $H^+HI(H_2O)_n$ in Figure 4.1.

The other species (HI^+, H^+HI, I_2^+, H^+I_2, $(HI)_2^+$, $H^+(HI)_2$) all result from ionization of the HI monomer or $(HI)_n$ clusters and the ensuing fragmentation of a H or I atom. Control experiments were performed with only $(HI)_n$ clusters to ensure the assignment of the growth seen in the I^+ species when water is present. The I^+, HI^+, and H^+ species exhibit plateaus or slight decays as shown in Figure 4.2, **A**, while the rest of the clusters show exponential decays. Thus the growth in the I^+ when water is present did not result from the pure $(HI)_n$ clusters.

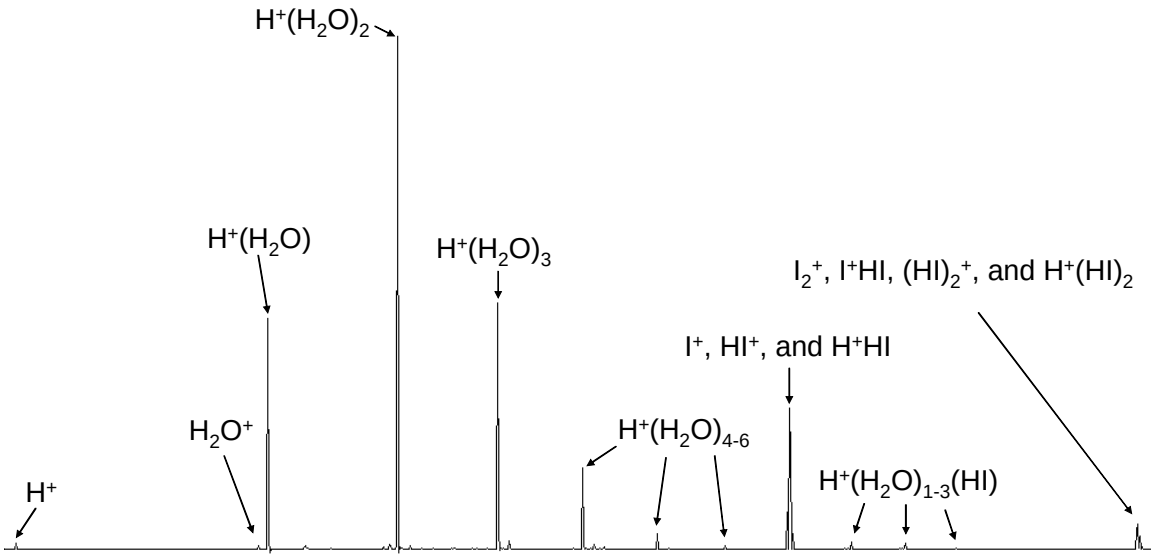

Figure 4.1. A mass spectrum of $HI(H_2O)_n$ clusters. Note that the $H(H_2O)_n^+$ clusters dominate the spectrum. The rise in the I^+ transient will only be observed when the population of the $H(H_2O)_n^+$ clusters is large in comparison to the $(HI)_n^+$ clusters.

As means to obtain a reliable transient length we performed experiments on HI monomer. At 200 nm excitation HI monomer predissociates to H and I atoms in less than the temporal response of our instrument. Since the growth of the I is instantaneous, as far as our experiment can measure, the only signal we see is a plateau in the I^+ transient and a cross-correlation in the HI^+ transient. The I atom is either spin excited or in the ground-state and the spin-excited state has a life time of over 0.1 seconds.[18] Thus, the I^+ should appear as a plateau in our experiment for all measurable timeframes as the growth appears instantaneous and the lifetime is near infinite on these time scales. Essentially, when our experiment no longer has overlap with the pump and probe beams we will not see the plateau in the I^+ of the HI monomer experiment. Doing this has shown us that our pump-probe experiment functions for a 400 picosecond window. Past 400 picoseconds we see a fall off in the I^+ plateau signal, as shown in Figure 4.3.

Figure 4.4 shows pump-probe transients of $H^+(H_2O)_n$ clusters from -1 to 300 picoseconds. Note the long rise in all of the clusters. A flat area is also seen in the

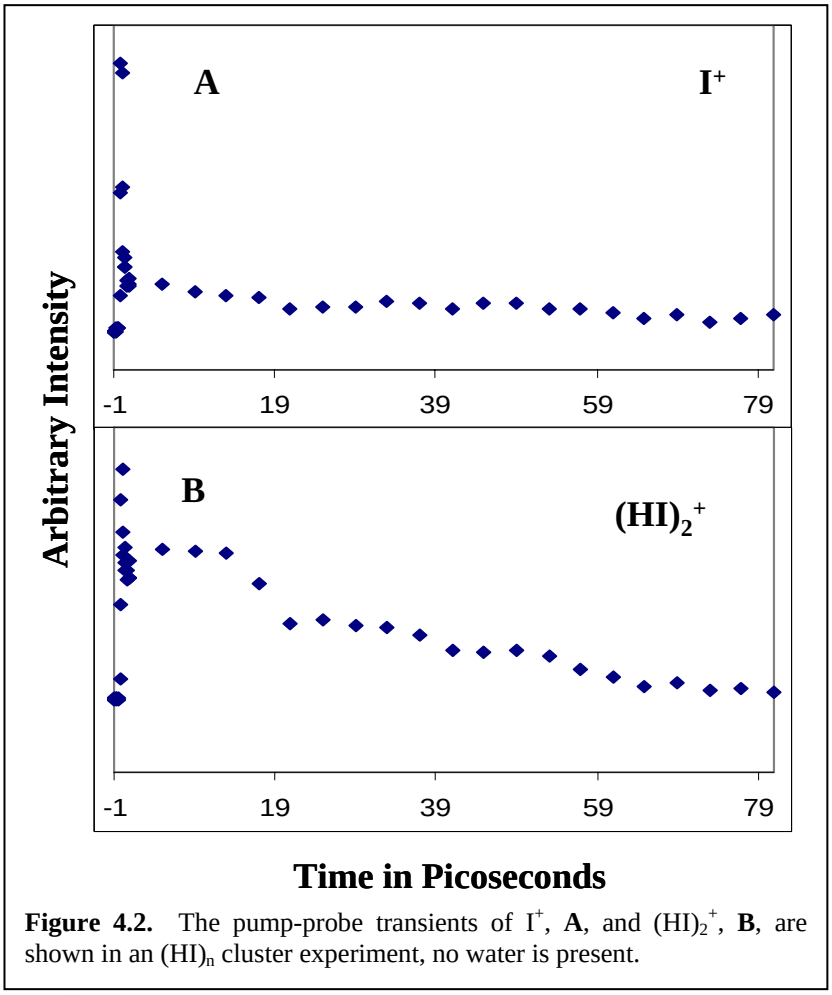

Figure 4.2. The pump-probe transients of I^+, **A**, and $(HI)_2^+$, **B**, are shown in an $(HI)_n$ cluster experiment, no water is present.

smaller ($n \leq 2$) $H^+(H_2O)_n$ cluster but not in the larger ($n > 2$). Also, the larger $H^+(H_2O)_n$ clusters seem to grow faster than the smaller ones. This observations can not be confirmed quantitatively as fitting these transients was unsuccessful due to their non-exponential behavior and the fact that we can not take a trace long enough to examine the entire process. The current incarnation of our experiment does not take a transient longer than about 400 picoseconds. However, we were able to readjust the overlap of the pump and probe beams at longer delays and perform power studies on the ionization process. The details of the power studies are discussed below.

The I^+ peak (see Figure 4.5) shows a growth similar to the $H^+(H_2O)_n$ clusters. As was discussed in Chapter 3, this I^+ signal originates from $HI(H_2O)_n$ clusters as was shown

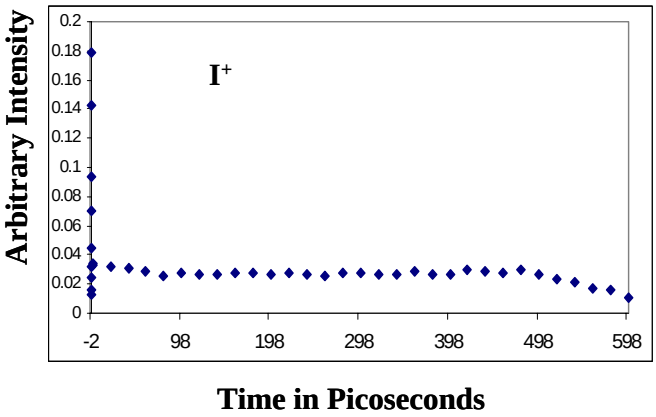

Figure 4.3. The pump-probe transients of the $HI(H_2O)_{1-6}$ clusters. Note the rise seen in all of the clusters. We were not able to take a pump-probe transient long enough to reveal all of the dynamics of these clusters, thus fitting them was not possible.

by the control experiments presented in Chapter 3. Thus, the fact that the I^+ transient qualitatively resembles the $H^+(H_2O)_n$ is not surprising.

Power studies were performed at various pump-probe delays to examine the change in ionization potential as the clusters evolve through time. The results are summarized in Table 4.1. The powers measured by our power meter are slightly off and when used as measured give photon counts that are clearly incorrect. For example, the ionization potential of the I atom is 10.45 eV and the energy of the probe is 3.1 eV; thus a photon count of 4 should be obtained from the power study. Previous experiments (see Chapter 3) have shown that the I atom dissociating from the $HI(H_2O)_n$ clusters is energetically similar to the I atom that dissociates from HI monomer. To correct for the slight errors in the measured power, the I^+ signal is used to internally calibrate the measured powers so that the photon count of I^+ comes out to be 4.

Figure 4.6 shows two plots of natural logarithm of probe laser power versus natural logarithm of signal intensity. The uncalibrated plot, **A**, uses the powers as measured from the power meter and the calibrated plot, **B**, where all the powers have had

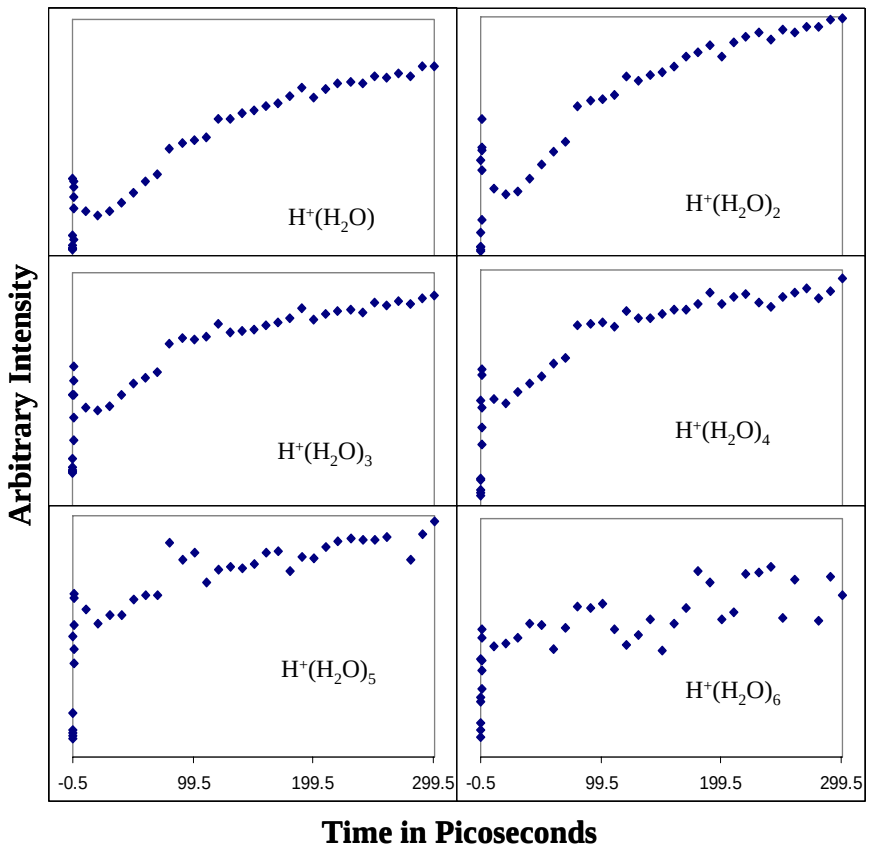

Figure 4.4. The pump-probe transients of the $HI(H_2O)_{1\text{-}6}$ clusters. Note the rise seen in all of the clusters. We were not able to take a pump-probe transient long enough to reveal all of the dynamics of these clusters, thus fitting them was not possible.

15 μJ/pulse subtracted to calibrate the photon count to 4. Note in **A**, the R^2 value of 0.9639 indicating good precision and linearity. Also note that the change in powers slightly improves the R^2 value. All of the powers used to obtain the photon counts reported in Table 4.1 have been calibrated to the I^+ signal to correct for the artifact in our power meter.

4.5 Discussion

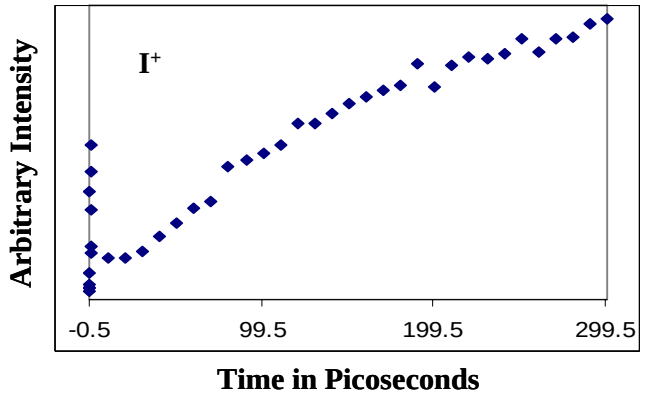

Figure 4.5. The pump probe transient of I^+. As discussed in Chapter 3 (Figure 3.2) the I^+ resembles the $H^+(H_2O)_n$ clusters.

Table 4.1 shows that the number of water molecules increases as the photon counts decreases. The $HI(H_2O)$ and $HI(H_2O)_2$ clusters ($n \leq 2$) both have higher photon counts, 4 and 3, respectively, than the larger $HI(H_2O)_n$ clusters ($n > 2$), which have photon counts of 2 or 1. From the ionization potential of HI (10.39 eV) and D_3O (4.3 eV), as well as the dissociation energy of HI (3.20 eV) we can make predictions as to how many photons will be necessary to ionize the clusters in our experiment. There are two general scenarios that could occur: the H-I bond could break, as occurs in the HI monomer, leaving an excess energy of 3.00 eV available as internal energy between the $H(H_2O)_n$ cluster and the I atom, or the cluster might stay intact, leaving all of the 6.2 eV of excitation energy available as internal energy.

If dissociation occurs, about 3.20 eV of the 6.2 eV of excitation energy will be lost to break the H-I bond. The 3.20 eV of dissociation energy for the HI monomer is a high estimate as solvation by water will lower the dissociation energy. Thus, 3.00 eV is available to both the $H(H_2O)_n$ cluster and I atom. The I atom has no more than 0.94 eV, leaving 2.11 eV of internal energy to the $H(H_2O)_n$ clusters. The ionization potential of

Table 4.1

Neutral	Detected	Ionization Potential	E_i	Photon Counts 250 ps	1000 ps	Expected	Known
H_2O	H_2O^+	12.621	0	4	4	4	4
$HI(H_2O)$	$H^+(H_2O)$	9.45-10.39	3.15-6.2	4	4	1 or 2	-
$HI(H_2O)_2$	$H^+(H_2O)_2$	9.45-10.39	3.15-6.2	3	3	1 or 2	-
$HI(H_2O)_3$	$H^+(H_2O)_3$	9.45-10.39	3.15-6.2	2	2	1 or 2	-
$HI(H_2O)_4$	$H^+(H_2O)_4$	9.45-10.39	3.15-6.2	2	2	1 or 2	-
$HI(H_2O)_5$	$H^+(H_2O)_5$	9.45-10.39	3.15-6.2	2	2	1 or 2	-
$HI(H_2O)_6$	$H^+(H_2O)_6$	9.45-10.39	3.15-6.2	1 or 2	1 or 2	1 or 2	-
I	I^+	10.45	0 or 0.94	4*	4*	4	4
$(HI)_2(H_2O)$	$H^+(HI)(H_2O)$	9.45-10.39	3.15-6.2	4 or 3	4 or 3	1 or 2	-
$(HI)_2(H_2O)_2$	$H^+(HI)(H_2O)_2$	9.45-10.39	3.15-6.2	2 or 3	2 or 3	1 or 2	-
$(HI)_2(H_2O)_3$	$H^+(HI)(H_2O)_3$	9.45-10.39	3.15-6.2	2	2	1 or 2	-

The results of our power studies at 250 and 1000 ps. The asterisks on the photon counts of I denote that it is used for calibration as the ionization potential is known. Note that the $HI(H_2O)$, $HI(H_2O)_2$, and $(HI)_2(H_2O)$ do not fit our predicted photon counts. E_i stands for internal energy, and the Expected column refers to two scenarios discussed in the text.

D_3O is 4.3 eV,[19] and we will assume that the ionization potential of the $H(H_2O)_n$ clusters is similar. Our probe photon energy is 3.1 eV, and combining this with the internal energy of the $H(H_2O)_n$ clusters gives us a total energy of 5.21 eV, well in excess of the energy needed to ionize D_3O. Thus, if the $HI(H_2O)_n$ cluster have dissociated their I atom we expect a one-photon count on the cluster.

If dissociation does not occur, all of the 6.2 eV of pump energy would be available as internal energy. The ionization potential of HI is 10.39 eV and the $HI(H_2O)_n$ clusters will have an ionization potential between the monomer and 9.45 eV from previous experiments.[2] Thus, 4.19 eV of energy is needed (10.39 eV - 6.2 eV= 4.19 eV) to ionize the $HI(H_2O)_n$ clusters, requiring two photons of the probe. From this analysis

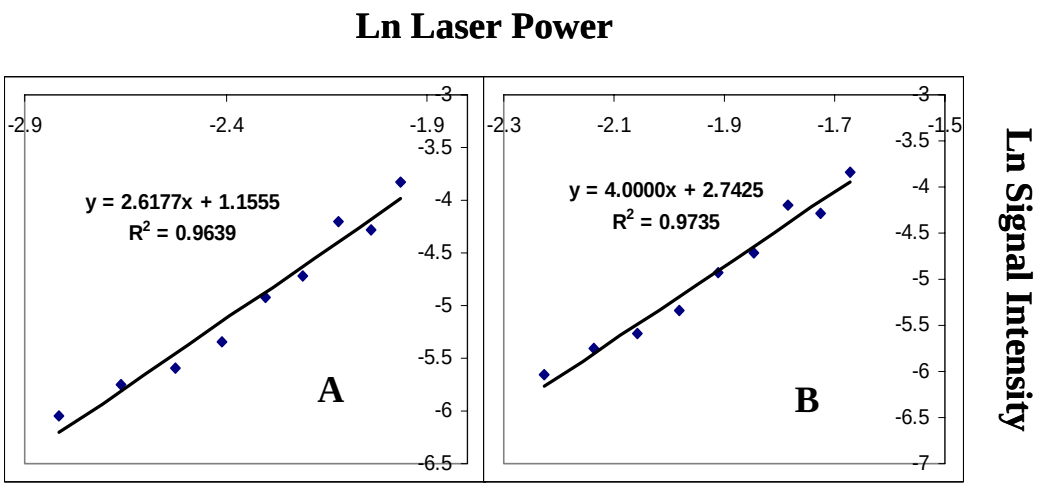

Figure 4.6. The before, **A**, and after, **B**, calibration of the power studies of the I^+ signal. The data are very linear in both cases, and the calibration actual improves the fit.

we conclude that the $HI(H_2O)_{3-5}$ are still intact and that the $HI(H_2O)_6$ has lost an I atom forming an $H(H_2O)_6$ cluster.

The $HI(H_2O)$, $HI(H_2O)_2$, and $(HI)_2(H_2O)$ clusters do not agree with these predictions and are not explained by the two scenarios above. They exibit higher photon counts than all the other $HI_m(H_2O)_n$ clusters in the mass spectrum. From previous experiments[4] we know that all the $H^+(H_2O)_n$ clusters started as $HI(H_2O)_n$ clusters before they are excited in our pump-probe experiment. Above we argue that if they have dissociated an I atom that their photon count should be one. Thus we must determine a scenario that involves the I atom associated with the cluster. Let us propose that the I atom is very loosely bound to the cluster as the dynamics of the I^+ transient lead us to believe. If this is the case, the cluster would have a power dependence similar to the lone I atom, as $HI(H_2O)$ does. This also suggest that perhaps some of the $HI(H_2O)$ clusters must have lost an I atom in the neutral state. The $H(H_2O)$ portion of the cluster can also interact with the probe laser, but this one- or two-photon interaction would overlap the four photon dependence of the $HI(H_2O)$ cluster with a loosely-bound I atom and would

not be seen in or experiment. From the power law equation then it is easy to see how this would occur:

$$\boldsymbol{I = P^{\lambda}}, \qquad \textbf{Equation 4.1}$$

where $\boldsymbol{I}$ is the signal intensity, $\boldsymbol{P}$ is the power, and $\boldsymbol{\lambda}$ is the photon count. If we look at the magnitude of signal from a $HI(H_2O)$ cluster with a loosely bound I atom, a four-photon process, at the lowest power used, 60 μJ/pulse, we get an arbitrary intensity of $(60\ \mu J/pulse)^4 = 1.296*10^7\ (\mu J/pulse)^4$, while an $H(H_2O)_n$ cluster with a two-photon dependence at the same power gives us an arbitrary intensity of $(60\ \mu J/pulse)^2 = 3.6*10^3\ (\mu J/pulse)^2$. Thus, a two-photon process that overlaps with a four-photon process would only affect signal in the fourth decimal place of the four-photon process. Therefore, we assign the $HI(H_2O)$, $HI(H_2O)_2$, and $(HI)_2(H_2O)$ clusters as having I atoms loosely attached at all times measure in these experiments. In the case of the $HI(H_2O)_2$, and $(HI)_2(H_2O)$ clusters, which have a photon count of three, we postulate that they represent some kind of intermediate structure from the very loosely bound $HI(H_2O)$ and the more strongly bound $HI(H_2O)_{3\text{-}6}$ clusters.

As discussed above the $HI(H_2O)_{1\text{-}2}$ and $(HI)_2(H_2O)$ clusters have higher photon counts because the I atom is not strongly associated with the cluster and the $HI(H_2O)_{3\text{-}5}$ have lower photon counts because the I atom is more strongly associated. There seems to be a threshold that is reached at the $HI(H_2O)_3$ cluster as the $HI(H_2O)_{4\text{-}5}$ clusters have the same photon count. However, the $HI(H_2O)_6$ has a photon count of one, indicating that I is dissociating from this clusters. How then do the clusters progress form having poorly associated I atom, to more strongly associated I atom, and then to dissociating an I atom?

This can be rationalized by examining the solvation effects that are occurring. The water molecules are dissolving the H-I bound into an H^+ and I^- in the ground-state and the water molecules are preferentially solvating the H^+ over the I^-. This is supported by the gas phase proton affinity of water (691 kJ/mol or 7.16 eV[20]) and the enthalpy of formation of an $I^-(H_2O)$ complex (46.44 kJ/mol or 0.4813 eV.[21]) If the excited-state is similar to the biradical as Chapter 3 supports, then there is some ionic character to the species we are observing. Additionally, H_3O is stabilized by water[22] so the H_3O moiety of the biradical, which has both ionic and radical character, will likely be preferentially solvated by water. Essentially, the H_3O^+/H_3O and I^-/I moieties are being separated in both the ground- and excited-state as water energetically favors solvation of the H_3O^+/H_3O moiety over the I^-/I moiety. Internal energy will increase as less and less of the pump energy is required to break the H-I bond. The decrease in photon counts as water is added could then represent ion-pair formation in the ground-state occurring in the $HI(H_2O)_3$ clusters as the drop in photon count levels off, staying the same in $HI(H_2O)_{3\text{-}5}$. Alternatively, it could represent the minimum amount of water molecules necessary for biradical formation in the excited-state. $HI(H_2O)_6$ cluster has a photon count of one most of the time, indicates dissociation of an I atom, due to the internal energy and solvation energy of the cluster having increased to the point where the I^-/I moiety is loosely bound.

4.6 Conclusions

We have shown that the addition of one water molecule to an HI can alter the nature of the potential energy surface from highly dissociative (HI monomer) to one that

is bound for at least 1 nanosecond for all $HI(H_2O)_n$ clusters. The $HI(H_2O)$, $HI(H_2O)_2$ and $(HI)_2(H_2O)$ clusters, though long lived, still show some dissociative character as the I atom associated with them appear poorly bound from the high photon counts of 3 and 4. The $HI(H_2O)_{3-5}$ and $(HI)_2(H_2O)_{2-3}$ clusters have the I atom more strongly associated with them and thus have different structure than the smaller clusters. These clusters are also long lived and thus stable. From the response we see at 1 nanosecond, we can estimate that all of the clusters in these studies must have lifetimes in that time regime. Given a lifetime in the nanosecond regime, processes like fluorescence are possible but are not measurable with our current instrumentation. The I atom dynamics suggests that at least some of the clusters are dissociating an I atom but only the $HI(H_2O)_6$ has a photon count that is consistent with I dissociation and not in all of our power studies. Thus it seems that the growth in the I atom originates from clusters with 6 or more water molecules. All of this evidence is in further support of a biradical structure proposed in Chapter 3. From conversations with Domcke, the I atom of the biradical structure will increase in bond length as the cluster is further solvated. Additionally, solvation will increase the internal energy of the cluster by weakening and eventually breaking the H-I bond, and all of the pump excitation energy would be available as internal energy. Thus the I atom evaporating from the larger $HI(H_2O)_6$ clusters is a reasonable interpretation. It should be noted that I atoms could be dissociating from smaller clusters but we can not observe them because signal from higher photon ionization processes would obscure the signal as discussed above.

With regards to ground-state ion-pair formation the decrease in photon count from the $HI(H_2O)$ to the $HI(H_2O)_3$ supports theoretical predictions that HI requires three water

molecule to form ion-pairs in the ground-state. The fact that the ion counts stay at two photons till the $HI(H_2O)_6$ would indicate that a threshold was reached at three water molecules. Another plausible interpretation is that this threshold represents the number of water molecules necessary to form the excited-state biradical. Thus our final interpretation of this system is as follows: the $HI(H_2O)$, $HI(H_2O)_2$ and $(HI)_2(H_2O)$ clusters might dissociate an I atom, however, we have strong evidence that some of the clusters have an I atom that is poorly bound to the cluster; the $HI(H_2O)_{3-5}$ and $(HI)_2(H_2O)_{2-3}$ clusters also have an I bound to them and might have been ground-state ion-pairs before excitation. The $HI(H_2O)_{6,}$ in some but not all of our power studies, appears to have dissociated an I atom from its photon count. This is a result of the $HI(H_2O)_6$ having the highest internal energy from a combination of pump excitation and solvation energy.

4.7 References

1. Hurley, S. M.; Dermota, T. E.; Hydutsky, D. P.; Castleman, A. W., Dynamics of hydrogen bromide dissolution in the ground and excited states. *Science* **2002,** 298, (5591), 202-204.
2. Dermota, T. E.; Hydutsky, D. P.; Bianco, N. J.; Castleman, A. W., Photoinduced ion-pair formation in the $(HI)_m(H_2O)_n$ cluster system. *Journal Of Chemical Physics* **2005,** 123, (21).
3. MacTaylor, R. S.; Gilligan, J. J.; Moody, D. J.; Castleman, A. W., Consideration of the bimolecular reaction rates of $D^+(D_2O)_n$ with HCl. *Journal Of Physical Chemistry A* **1999,** 103, (15), 2655-2658.
4. Hurley, S. M.; Dermota, T. E.; Hydutsky, D. P.; Castleman, A. W., The ultrafast dynamics of HBr-water clusters: Influences on ion-pair formation. *Journal Of Chemical Physics* **2003,** 118, (20), 9272-9277.
5. Raymond, E. A.; Richmond, G. L., Probing the molecular structure and bonding of the surface of aqueous salt solutions. *Journal Of Physical Chemistry B* **2004,** 108, (16), 5051-5059.

6. Knipping, E. M.; Lakin, M. J.; Foster, K. L.; Jungwirth, P.; Tobias, D. J.; Gerber, R. B.; Dabdub, D.; Finlayson-Pitts, B. J., Experiments and simulations of ion-enhanced interfacial chemistry on aqueous NaCl aerosols. *Science* **2000,** 288, (5464), 301-306.
7. Kazil, J.; Lovejoy, E. R.; Barth, M. C.; O'Brien, K., Aerosol nucleation over oceans and the role of galactic cosmic rays. *Atmospheric Chemistry And Physics* **2006,** 6, 4905-4924.
8. Sobolewski, A. L.; Domcke, W., Photochemistry of water: The $(H_2O)_5$ cluster. *Journal Of Chemical Physics* **2005,** 122.
9. Verlet, J. R. R.; Bragg, A. E.; Kammrath, A.; Cheshnovsky, O.; Neumark, D. M., Observation of large water-cluster anions with surface-bound excess electrons. *Science* **2005,** 307, (5706), 93-96.
10. Headrick, J. M.; Diken, E. G.; Walters, R. S.; Hammer, N. I.; Christie, R. A.; Cui, J.; Myshakin, E. M.; Duncan, M. A.; Johnson, M. A.; Jordan, K. D., Spectral signatures of hydrated proton vibrations in water clusters. *Science* **2005,** 308, (5729), 1765-1769.
11. Turi, L.; Sheu, W. S.; Rossky, P. J., Characterization of excess electrons in water-cluster anions by quantum simulations. *Science* **2005,** 309, (5736), 914-917.
12. Hammer, N. I.; Shin, J. W.; Headrick, J. M.; Diken, E. G.; Roscioli, J. R.; Weddle, G. H.; Johnson, M. A., How do small water clusters bind an excess electron? *Science* **2004,** 306, (5696), 675-679.
13. Paik, D. H.; Lee, I. R.; Yang, D. S.; Baskin, J. S.; Zewail, A. H., Electrons in finite-sized water cavities: Hydration dynamics observed in real time. *Science* **2004,** 306, (5696), 672-675.
14. Goyal, S.; Robinson, G. N.; Schutt, D. L.; Scoles, G., Infrared-Spectroscopy Of SF_6 In And On Argon Clusters In An Extended Range Of Cluster Sizes - Finite-Size Particles Attaining Bulk-Like Properties. *Journal Of Physical Chemistry* **1991,** 95, (11), 4186-4189.
15. Gough, T. E.; Knight, D. G.; Scoles, G., Matrix Spectroscopy In The Gas-Phase - Ir Spectroscopy Of Argon Clusters Containing SF_6 Or CH_3F. *Chemical Physics Letters* **1983,** 97, (2), 155-160.
16. Bergmann, T.; Goehlich, H.; Martin, T. P.; Schaber, H.; Malegiannakis, G., High-Resolution Time-Of-Flight Mass Spectrometers.2. Cross Beam Ion Optics. *Review Of Scientific Instruments* **1990,** 61, (10), 2585-2591.
17. Bergmann, T.; Martin, T. P.; Schaber, H., High-Resolution Time-Of-Flight Mass Spectrometers.2. Reflector Design. *Review Of Scientific Instruments* **1990,** 61, (10), 2592-2600.
18. Chichinin, A. I., Chemical properties of electronically excited halogen atoms $X(^2P_{1/2})$ (X=F,Cl,Br,I). *Journal Of Physical And Chemical Reference Data* **2006,** 35, (2), 869-928.
19. Gellene, G. I.; Porter, R. F., Experimental-Evidence For Metastable States Of D3o And Its Monohydrate By Neutralized Ion-Beam Spectroscopy. *Journal Of Chemical Physics* **1984,** 81, (12), 5570-5576.
20. Hunter, E. P. L.; Lias, S. G., Evaluated gas phase basicities and proton affinities of molecules: An update. *Journal Of Physical And Chemical Reference Data* **1998,** 27, (3), 413-656.

21. Keesee, R. G.; Castleman, A. W., Gas-Phase Studies Of Hydration Complexes Of Cl- And I- And Comparison To Electrostatic Calculations In The Gas-Phase. *Chemical Physics Letters* **1980,** 74, (1), 139-142.
22. Gellene, G. I.; Porter, R. F., A Study Of The Target Gas Dependence On The Collisional Ionization Mass-Spectra Of Some Metastable And Hypervalent Molecules. *International Journal Of Mass Spectrometry And Ion Processes* **1985,** 64, (1), 55-66.

Chapter 5

Photodissociation of SO_2 Between 200 and 197 nm

5.1 Abstract

Pump-probe experiments on the C state of SO_2 have been performed to assess the details of the oxygen photodissociation process between 197 and 200 nm. Our interpretation is as follows: a prompt dissociation event occurs in less than 265 but more than 100 femtoseconds; a reorganization of internal energy occurs in 15 or 28 picoseconds depending on the excitation energy: the change in lifetime represents contributions from asymmetric vibrational states seen in previous experiments, and a long lived species (lifetime >> 60 picoseconds) exists that does not decay on the timeframe of our experiment. We discuss these findings with regard to previous studies and the avoided crossing in this region of the potential energy surface of SO_2.

5.2 Introduction

Interrogating the potential energy surfaces of small molecules facilitates the advancement of spectroscopic techniques and refinement of computational methods. Extensive research on the C state of SO_2 has been performed to aid in the interpretation of the mechanisms of oxygen dissociation.[1-9] These efforts have taken place over a period of decades [9] and a comprehensive review of the photodissociation of SO_2 exists[5].

SO_2 has been extensively studied to understanding its fate in our atmosphere.[10] Through reactions within aerosol particles and several oxidizers in the atmosphere, SO_2 is converted into sulfuric acid. Sulfuric acid is a very important molecule in nucleation phenomena,[11] producing ultrafine particles that grow into aerosol particles. These aerosol particles are of great interest, as well, because of the role they play in cloud formation and the energy budget of the Earth.[12] Sulfuric acid is also one of the large contributors to acid rain. There are naturally occurring sources of SO_2 and other sulfur containing species (H_2S and DMS for example), but large amounts of SO_2 also are emitted from anthropogenic sources.[13]

Our group[2, 14-18] has undertaken an extensive study of both bound and dissociative processes in SO_2, and how clustering can affect these processes. These studies have revealed a wealth of information on the chemical behavior of electronically excited SO_2 and how solvation affects these properties. Recent studies[19, 20] have shown that SO_2 attaches at the air water interface, thus validating our cluster methods for examining how solvation can affect the chemistry of atmospherically relevant molecules.

By studying the dynamics of SO_2 excited by 200-197 nm light, we add to the interpretation of photochemical dissociation studies. Our experiments have examined several path ways in the photo-dissociation process: prompt dissociation of SO_2; redistribution of energy through an avoided crossing; a drop in the lifetime of the redistribution of energy through an avoided crossing near an excitation energy of 198 nm and a long lived SO_2 species that persists for longer than the time frame of our experiment (60 picoseconds) that coincides with the drop in the above mentioned redistribution energy.

5.3 Experimental

The instrument used in these experiments consists of a femtosecond laser system that produces 100 fs pulses, at 10 Hz, with 2.5 mJ per pulse, centered at 800 nm. The fundamental is frequency doubled and mixed to produce second, third, and fourth harmonics. The second harmonic was used in all cases for the probe beam and the fourth harmonic was used for the pump beam. The system is slightly tunable and specific wavelengths for specific experiments are given in the text. Both pure SO_2 and mixtures of SO_2 and helium were introduced by a Parker solenoid valve and a pick-up source.[21, 22] No discernable difference between introduction through the solenoid and the pick-up source was observed. We used low backing pressure (less than one atm) and pulse nozzle conditions that are not conducive to clustering. No clusters were observed in the mass spectrum and we conclude from this that no SO_2 clusters were present in our experiments. Detection of ionized species was performed with a home-built time-of-flight mass spectrometer consisting of a quadrapole time-of-flight assembly[23] a reflection,[24] and a Burle bipolar detector. Signal from the detector was acquired by a Tektronics oscilloscope model TDS5104B.

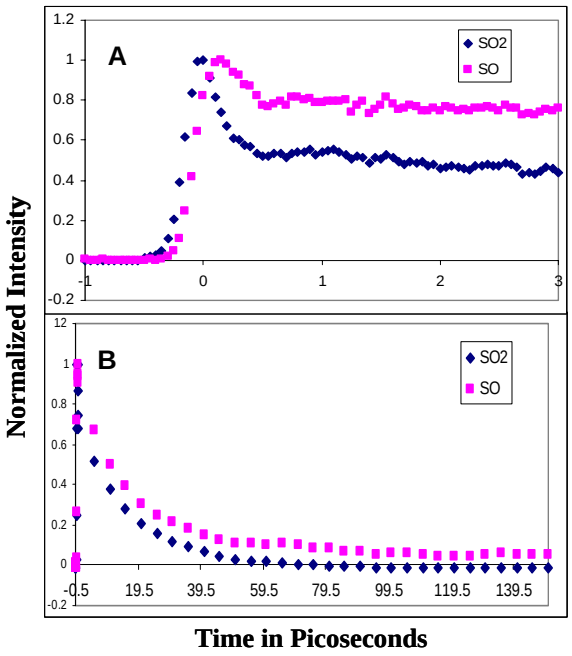

Figure 5.1. The pump-probe transient of SO_2 and SO from -2 to 3 picoseconds are shown, **A,** and out to 150 picoseconds, **B.**

Figure 5.1 shows a typical pump-probe transient of SO_2 in the first few picoseconds, **A**, and at longer delays, **B**. All pump-probe transients shown in this paper have been baseline corrected using the time dynamics before the zero, and normalized to the highest intensity point in the pump-probe transient. The SO_2 transients can consist of as many as three components. In order of increasing lifetime: a fast decay component, $\boldsymbol{I_f}$, a slow decay component, $\boldsymbol{I_s}$, with a 15 to 28 ps lifetime depending on the excitation wavelength, and a component that does not change on the time scale of our experiment, $\boldsymbol{I}_{p,}$ that we will refer to as a plateau. The fitting equation used is adapted from previous work[25] and is of the following form:

$$I_T = I_f + I_s + I_p + a\,, \qquad \textbf{Equation 5.1}$$

here $\boldsymbol{I_T}$ is the total signal intensity, $\boldsymbol{a}$ accounts for background signal, and all other components are discussed above. $\boldsymbol{I_f}$ and $\boldsymbol{I_s}$ are of the following form:

$$I_n(t,\tau_n) = \mathrm{c_n}\left[1 - erf\left\{\frac{\sigma}{2*\tau_n} - \frac{t+c}{\sigma}\right\}\right] * \exp\left\{\left(\frac{\sigma}{2*\tau_n}\right)^2 - \frac{t+c}{\tau_n}\right\}, \qquad \textbf{Equation 5.2}$$

where $\boldsymbol{c_n}$ represents the amplitude of the component, $\boldsymbol{\sigma}$ represents the instrument response, $\boldsymbol{\tau_n}$ represents the lifetime of the component in question, $\boldsymbol{t}$ represents the delay between the pump and probe pulse, and $\boldsymbol{c}$ is a parameter used to account for any slight mismatches of the assigned zero of the experiment. Many efforts were made to fit the fast decay dynamics to a decay function but the reliability of the fits were poor, and the dynamics extracted were faster than the temporal response of our instrument. However, a short-time component is present in each fitting function to account for the amplitude produced near the zero. Time zero is defined as the maximum intensity of Xenon gas and is discussed in the results section. The numbers that are produced by fast decay fits are not given consideration because of their inconsistent nature; they are present in the fitting equation only to account for the intensity near the zero of the experiment. In fact, when the fast component of the fitting equation was replaced with a Gaussian function to account for the intensity produced at the zero of the experiment, no appreciable change was observed in the fit. We do have other evidence for an estimate of what the dissociation time is for SO_2 excited by these energies, and they are examined in the results and discussion sections. In the case of $\boldsymbol{I_p}$ where the signal does not decay in the timeframe of our experiment, we represent this amplitude with the limit of Equation 5.2 as $\boldsymbol{\tau_n}$ goes to infinity:

$$I_n(t,\tau_n) \xrightarrow[\lim \tau \to \infty]{} I_p(t) = \left[1 - erf\left\{-\frac{t+c}{\sigma}\right\}\right], \qquad \textbf{Equation 5.3}$$

the plateau component is only used when there is signal in the pump-probe transient that does not decay. Put simply, if you can not see the plateau from a visual inspection of the transient, the fitting equation will not be able to assign the correct amplitude. Thus, in the shorter time-scale transient, the plateau is not included.

5.4 Results

Time zero for the experiment was determined by adding a small amount of Xe gas in with the SO_2, as seen in Figure 5.2. Time zero for the experiment is found to be 100 femtoseconds before the peak signal for the SO_2^+ species, and 200 femtoseconds before the peak signal for the SO^+ species. Additionally, the full-width-at-half-maximum signal of the Xe^+ transient is used as a measure of the instrument response time for these harmonics and wavelengths. We find that our instrument response time is 265 femtoseconds. If the fast decay is less than 265 femtoseconds, as it appears to be, then we will not be able to obtain direct measurements. In the discussion section we will justify that there is a fast decay, as well as bracket the life time of the fast decay.

The effect of changing the polarization of the pump and probe beam with respect to each other has been reported in previous work.[26] In summary, we found that ion-state fragmentation is the only response seen in the SO^+ species when the pump and probe beam are polarized perpendicular to each other. When the polarization is parallel, a difference in the SO^+ and SO_2^+ dynamics is observed. We interpret this as evidence that

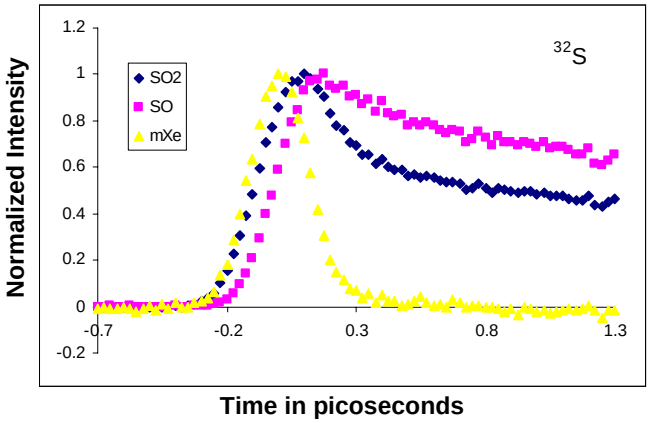

Figure 5.2. The transients of Xenon, SO_2, and SO. Note that the SO_2 is shifted to later time from the Xenon and the SO is shifted further.

the O that dissociates from SO_2 is not the O that is in line with the polarization of the pump pulse. This would leave the excited SO moieties in line with the probe when the laser pulses are in a parallel configuration. Thus, in the parallel configuration the excited SO moiety can be easily ionized because of the alignment of the molecule to the polarization on the probe beam. In the perpendicular configurations, only ion-state fragmentation is seen because the probe beam is interacting with an intact SO_2 molecule that has one of the O atoms close to the polarization of the probe laser. The vibrational and rotational excitation of the SO should also be taken into consideration and is discussed below.

Higher powers also cause ion-state fragmentation of the SO_2^+ into SO^+ and O. The details of the process are shown in Table 5.1. The two photons of ~ 400 nm light, needed to ionize the excited SO_2, is a resonant process that goes through the F band[17] to the ion-state. As shown in Table 5.1, the absorption of four photons is also possible. The dynamics of the ion-fragment (SO^+) will be the same as the dynamics of the parent ions (SO_2^+). Thus at higher powers, where ion-state fragmentation is dominant, the dynamics

of SO^+ may appear the same as the dynamics of SO_2^+, as seen in Figure 5.3, **A**. At lower powers, the ion-state fragmentation is still present but differences can be seen, in Figure

Table 5.1 Reaction	Process	Energy Added	Total Energy	Required
$SO_2 + \lambda_{200nm} \rightarrow SO_2^*$	Pump to C state	6.20-6.30 eV	6.20-6.30 eV	5.6-7.4 eV
$SO_2^* + \tau \rightarrow SO + O$	Dissociation	0 eV	6.20-6.30 eV	5.65 eV
$SO_2^* + 2\lambda_{400nm} \rightarrow SO_2^+ + e^-$	C State Dynamics of SO_2^*	6.20-6.30 eV	12.40-12.60 eV	12.35 eV
$SO_2^* + 4\lambda_{400nm} \rightarrow SO^+ + O$	Ion-state Fragmentation	12.40-12.60 eV	18.60-18.90 eV	15.93 eV
$SO + 4\lambda_{400nm} \rightarrow SO^+ e^-$	Ground-state Dynamics of SO	12.40-12.60 eV	12.40-12.60 eV	10.29 eV

This table summarizes the processes that are occurring in our experiment. All energies are in eV.

5.3, **B**, between the SO^+ and SO_2^+ species. This difference is thought to be the neutral-state dynamics of the ground electronic state SO species. Our rationale for why the difference of the SO^+ and SO_2^+ can be viewed as the qualitative analysis of the neutral SO fragment is given in the discussion section. Note that efforts were made to reduce probe power to the point where only the dynamics of neutral-state SO are seen, but ion-state fragmentation requires the same number of photons as ionization of SO (see Table 5.1). To give a qualitative feel for the dynamics of the ground electronic state of the SO fragment, difference spectra of baseline and normalized SO^+ and SO_2^+ are subtracted (SO^+ - SO_2^+) from each other as shown in Figure 5.3, **C**. The dip in the transient is due to the difference in peak-intensity time of the SO_2^+ and SO^+ signal. The difference in peak-intensity time can be taken as evidence of the neutral state dissociation of SO_2 into SO and O as discussed later. We view these difference spectra as yielding a purely qualitative picture of the dynamics of vibrationally excited neutral SO, and no attempt was made to fit these transients.

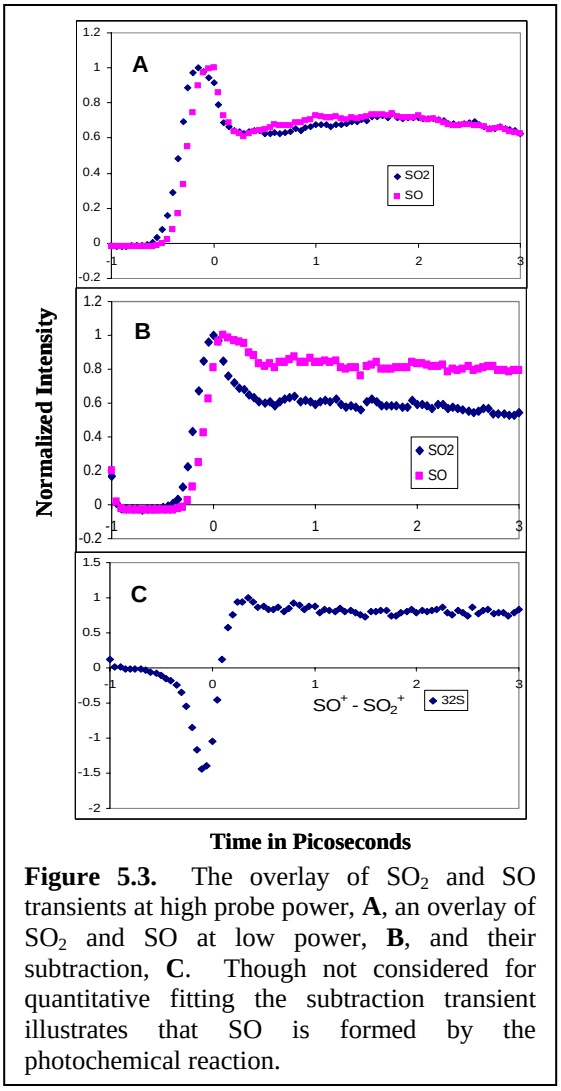

Figure 5.3. The overlay of SO_2 and SO transients at high probe power, **A**, an overlay of SO_2 and SO at low power, **B**, and their subtraction, **C**. Though not considered for quantitative fitting the subtraction transient illustrates that SO is formed by the photochemical reaction.

The pump wavelength can have a pronounced effect on the lifetime of the long decay, as seen in Figure 5.4. The life time of the long decay drops from 28 picoseconds at 199.5 nm to 15 picoseconds at 197.5 nm. Additionally, at 197.5 nm, a plateau can be seen at long times in the spectra. These results are discussed later, with respect to asymmetric stretches and the avoided crossing, in the discussion section.

S^+ and O^+ are observed in some of the mass spectra, especially at high probe powers. The pump-probe transients of these species are identical to the SO_2^+ species for all probe powers studied. We conclude from this observation, that these species are products of ion-state fragmentation. No evidence of neutral-state S or O can be extracted

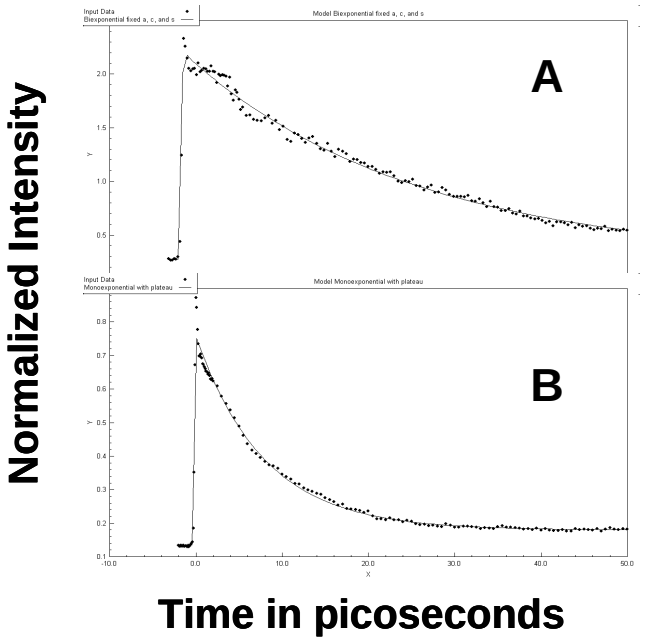

Figure 5.4. The difference in lifetimes when the pump wavelength is 199.5 nm, **A**, versus 197.5 nm, **B**.

from the observation of these species. Metastable peaks that track with the SO^+ peak are seen in many of the mass spectra, which suggest that the SO^+ species contains enough internal energy to further dissociate another O. However, since the dynamics are the same as the SO_2^+ species, the additional energy to dissociate the second O must have originated form the probe pulse.

5.5 Discussion

As stated in the results section, no reliable fitting information could be obtained for the prompt dissociation of SO_2. However, there is evidence for a prompt dissociation of SO_2. Examining the response of the SO fragment, we see from Figure 5.3 that at low power significant differences between the parent SO_2 and the SO fragment are readily apparent. At higher probe power, ion-state fragmentation is clearly occurring. This is evident by the fact that the pump-probe transients of SO_2 and SO overlay each other

almost perfectly (Figure 5.3, **A**) once they are baselined and normalized. Thus, ion-state fragmentation is competitive with the process that occurs at lower probe energies as Table 5.1 indicates. The question then is whether the SO fragment is electronically excited or not? The dissociation energy, D_e, for SO_2 ➔ SO + O is 5.65 eV and the lowest electronic excited-state of the SO fragment is 0.75 eV. The combined energy is 6.4 eV, higher than the excitation energy of the pump pulse (6.3 eV) at the highest energy used. Additionally, studies[4, 27] that examined the photodissociation products formed at 6.4 eV found no evidence of electronically excited SO, only ground-state vibrationally excited products. Thus we can rule out electronically excited SO based energy analysis and previous experiments by other groups.

We then have ground-state SO competing with ion-state fragmentation as a likely candidate, but let us look at the energetics of both processes. Table 5.1 shows many of the photochemical processes that are taking place in our experiment along with the energies supplied by the pump and probe beams as well as the energy required for these processes to occur. We can see from this energy analysis that both ionization of ground-state SO and ion-state fragmentation are indeed competitive as they both require four probe photons. Additionally, polarization studies from a previous work[26] show that with the pump and probe beam perpendicular, no neutral SO^+ dynamics are seen, only ion-state fragmentation. The polarization studies show that the orientation of the fragment to the probe laser is indeed important for the neutral process but not for ion-state fragmentation. SO_2 is a bent molecule and we assume that the pump laser preferentially excites molecules with one of the S-O bonds parallel to the polarization of the pump beam. Assuming that the S-O fragment is oriented parallel to the polarization of the

probe laser is reasonable given dipole considerations in electronic excitation processes. Additionally, the vibrational spectrum of the SO fragment has been measured near these excitation energies.[27] We can now understand the physical phenomena behind these observations. After excitation, an intact SO_2 molecule can interact with the probe beam in a perpendicular or parallel polarization because of the bent structure of the SO_2 molecule. If a dissociation event occurs, one of the O atoms will fall off, leaving a linear SO molecule. Depending on which O atom dissociates, the polarization of the probe beam will affect ionization efficiency. Since we only see evidence of neutral SO when the polarization of the probe beam is parallel to the pump beam, the dissociation event must take place on the S-O bond that is nearly perpendicular to the polarization of the pump beam.

We conclude that there is a fast dissociation that produces ground-state SO. Additionally, the SO fragment does decay with time, so though we know that there is not sufficient energy for an electronic excitation, vibrational and rotational excitations are possible. Previous work[4, 27] again provides further evidence, as these experiments measured the vibrational and rotational distributions of the SO fragment and indeed found that the SO fragments are vibrationally and rotationally excited.

Why then did our attempts to fit the data with a fast decay produce nearly identical results to fitting attempts that included a Gaussian function to account for enhancement near the zero? Earlier measurements in our group[16] for excitation at 8 eV showed the dissociation of SO_2 to be 230 fs. As stated in the results section, our instrument response is 265 femtoseconds, thus explaining why we cannot obtain direct measurements of the fast dissociation if we assume that the dissociation time for the C

state is similar. The delay in the SO^+ transient of 100 femtoseconds, compared to the SO_2^+ transient, is interpreted as indirect evidence of a fast dissociation. No measurable growth is seen in the SO^+ transient data, as expected, since the dynamics in the parent are faster than the instrument response. Thus, we suggest that upon excitation there is a fast channel that dissociates SO_2 into ground-state SO detectable by four photons of 3.15 eV probe in less than 265 femtoseconds but no faster than the 100 femtosecond offset of the SO^+ transient at low probe power. We assign a four probe photon ionization process (12.4-12.6 eV) from the known ionization energies of ground-state SO (10.29 eV) and the fact that the dynamics we see are competitive with ion-state fragmentation, which also requires four photons of the probe.

The slow decay seen in Figure 5.4 of SO_2^+ chromophore has strong pump wavelength dependence, with an abrupt change in the life time occurring at ~ 198 nm. In the results section, it was noted that at this energy the slow decay time drops from 28 picoseconds to 15 picoseconds. This abrupt drop roughly coincides with the onset of population in asymmetric stretches of the SO_2 chromophore in previous experiments[3]. The fact that this causes the lifetime to significantly decrease, strongly suggests that this process involves the avoided crossing near the dissociation threshold of 5.66 eV, as asymmetric stretches will break symmetry constraints, allowing population to move faster through the avoided crossing.

A similar decay is seen in the SO^+ fragment, though measurements are not available due to issues with ion-state fragmentation (see Results section). The SO^+ fragment is vibrationally and rotationally excited, as previous work has shown;[4, 27] thus, the long dynamics seen in the SO^+ can immediately be assigned to internal redistribution

of energy throughout the vibrational and rotational modes. As the lifetime of the long decay is on the same order of magnitude as the rotational constant it seems reasonable to more specifically assign the long decay as redistribution within the rotational modes of the SO fragment. Also, no second growth is seen in the SO^+ fragment; thus, there is no evidence that the long decay in the SO_2^+ chromophore representing a dissociative process. If a dissociative process is occurring in the long decay, then the product SO of this decay is not detectable by this experiment.

The plateau seen in our transients represents an SO_2 species with a very long-life, time and no signs of decay are seen in our experiment. The plateau only appears in spectra where the pump wavelength is 198 nm or lower, and coincides with the drop of the long decay from 28 to 15 picoseconds. From our interpretation of the long decay component discussed above, this long-lived state must be the result from population transfer to a bound state with a lower absorption cross-section than the originally excited state. The transients at lower energy (199 nm) decay below the background signal from the probe beam.

5.6 Conclusion

Our interpretation is summarized below.

$SO_2 + h\nu_{200nm}$ ➔ SO + O [Prompt dissociation (100-265 femtoseconds)]

➔ SO_2^* [Internal redistribution of energy through avoided crossing (15 or 28 ps depending on excitation energy)]

➔ SO_2^* [Bound state (>> 60 ps)]

There is no evidence in our experiment for a second dissociation of atomic oxygen, only the prompt dissociation that occurs between 100 and 265 femtoseconds. As to the ongoing debate on whether the dissociation pathway is a singlet or triplet,[3, 28] our results do not indicate singlet or triplet, but do suggest that only one dissociative event occurs. The change in the lifetime of the long decay fits well with the onset of asymmetric stretches[3, 28] in the emission spectra at these energies. The concomitant appearance of the plateau at higher excitation energies is perplexing and seems to suggest that the population is evolving to dark state above the onset of asymmetric stretches. The population could then goes to a bright state once asymmetric stretches change the symmetry, where at first the population proceeded to a dark state. This scenario is certainly plausible as emissions from SO_2 excited by these energies have been measured[3, 28] for excitation energies of lower energy than those used here.

Future studies will investigate how clustering affects the mechanisms seen in this study. If past experiments are relevant,[15] only a small amount of clustering should be needed to shut off the dissociative mechanism. Clustering could break the symmetry of the chromophore before the experiment begins, thus we would not expect to see the same change in the lifetime of the long decay component. Also, as the symmetry would be broken, the long plateau seen in these experiments should be present in the clusters.

5.7 References

1. Jung, S.; Tiemann, E.; Lisdat, C., The Stark effect of the excited C^1B_2 state of SO_2 and manipulation of dissociation channels. *Journal Of Physics B-Atomic Molecular And Optical Physics* **2006,** 39, (19), S1085-S1095.
2. Hurley, S. M.; Dermota, T. E.; Hydutsky, A. P.; Castleman, A. W., Photodissociation of SO_2 clusters. *Journal Of Physical Chemistry A* **2003,** 107, (18), 3497-3502.
3. Ray, P. C.; Arendt, M. F.; Butler, L. J., Resonance emission spectroscopy of predissociating SO_2 C $^1B_2$: Coupling with a repulsive (1)A(1) state near 200 nm. *Journal Of Chemical Physics* **1998,** 109, (13), 5221-5230.
4. Braatz, C.; Tiemann, E., State-to-state dissociation of SO_2 in C $^1B_2$: Rotational distributions of the fragment SO. *Chemical Physics* **1998,** 229, (1), 93-105.
5. Katagiri, H.; Sako, T.; Hishikawa, A.; Yazaki, T.; Onda, K.; Yamanouchi, K.; Yoshino, K., Experimental and theoretical exploration of photodissociation of SO2 via the C $^1B_2$ state: identification of the dissociation pathway. *Journal Of Molecular Structure* **1997,** 413, 589-614.
6. Becker, S.; Braatz, C.; Lindner, J.; Tiemann, E., Investigation Of The Predissociation Of SO_2: State-Selective Detection Of The SO Fragment And O Fragment. *Chemical Physics* **1995,** 196, (1-2), 275-291.
7. Becker, S.; Braatz, C.; Lindner, J.; Tiemann, E., State-Specific Photodissociation Of SO_2 And State-Selective Detection Of The So Fragment. *Chemical Physics Letters* **1993,** 208, (1-2), 15-20.
8. Ahmed, S. M.; Kumar, V., Quantitative Photoabsorption And Fluorescence Spectroscopy Of SO_2 At 188-231nm And 278.7-320nm. *Journal Of Quantitative Spectroscopy & Radiative Transfer* **1992,** 47, (5), 359-373.
9. Warneck, P.; Sullivan, J. O.; Marmo, F. F., Ultraviolet Absorption Of SO_2: Dissociation Energies Of SO_2 + SO. *Journal Of Chemical Physics* **1964,** 40, (4), 1132-&.
10. Laj, P.; Fuzzi, S.; Facchini, M. C.; Orsi, G.; Berner, A.; Kruisz, C.; Wobrock, W.; Hallberg, A.; Bower, K. N.; Gallagher, M. W.; Beswick, K. M.; Colvile, R. N.; Choularton, T. W.; Nason, P.; Jones, B., Experimental evidence for in-cloud production of aerosol sulphate. *Atmospheric Environment* **1997,** 31, (16), 2503-2514.
11. Kazil, J.; Lovejoy, E. R.; Barth, M. C.; O'Brien, K., Aerosol nucleation over oceans and the role of galactic cosmic rays. *Atmospheric Chemistry And Physics* **2006,** 6, 4905-4924.
12. Li, J.; Wong, J. G. D.; Dobbie, J. S.; Chylek, P., Parameterization of the optical properties of sulfate aerosols. *Journal Of The Atmospheric Sciences* **2001,** 58, (2), 193-209.
13. Alfonso, L.; Raga, G. B., Estimating the impact of natural and anthropogenic emissions on cloud chemistry. Part 1. Sulfur cycle. *Atmospheric Research* **2002,** 62, (1-2), 33-55.
14. Zhong, Q.; Hurley, S. M.; Castleman, A. W., Dissociation pathways of sulfur dioxide clusters and mixed sulfur dioxide water clusters. *International Journal Of Mass Spectrometry* **1999,** 187, 905-911.
15. Knappenberger, K. L.; Castleman, A. W., The influence of cluster formation on the photodissociation of sulfur dioxide: Excitation to the E state. *Journal Of Chemical Physics* **2004,** 121, (8), 3540-3549.

16. Knappenberger, K. L.; Castleman, A. W., Photodissociation of sulfur dioxide: The E state revisited. *Journal Of Physical Chemistry A* **2004,** 108, (1), 9-14.
17. Dermota, T. E.; Hydutsky, A. P.; Bianco, N. J.; Castleman, A. W., Excited-state dynamics of $(SO_2)_m$ clusters. *Journal Of Physical Chemistry A* **2005,** 109, (37), 8259-8267.
18. Dermota, T. E.; Hydutsky, D. P.; Bianco, N. J.; Castleman, A. W., Ultrafast dynamics of the $SO_2(H_2O)_n$ cluster system. *Journal Of Physical Chemistry A* **2005,** 109, (37), 8254-8258.
19. Tarbuck, T. L.; Richmond, G. L., Adsorption and reaction of CO_2 and SO_2 at a water surface. *Journal Of The American Chemical Society* **2006,** 128, (10), 3256-3267.
20. Tarbuck, T. L.; Richmond, G. L., SO_2: H_2O surface complex found at the vapor/water interface. *Journal Of The American Chemical Society* **2005,** 127, (48), 16806-16807.
21. Goyal, S.; Robinson, G. N.; Schutt, D. L.; Scoles, G., Infrared-Spectroscopy Of SF_6 In And On Argon Clusters In An Extended Range Of Cluster Sizes - Finite-Size Particles Attaining Bulk-Like Properties. *Journal Of Physical Chemistry* **1991,** 95, (11), 4186-4189.
22. Gough, T. E.; Knight, D. G.; Scoles, G., Matrix Spectroscopy In The Gas-Phase - Ir Spectroscopy Of Argon Clusters Containing SF_6 Or CH_3F. *Chemical Physics Letters* **1983,** 97, (2), 155-160.
23. Bergmann, T.; Goehlich, H.; Martin, T. P.; Schaber, H.; Malegiannakis, G., High-Resolution Time-Of-Flight Mass Spectrometers Part II. Cross Beam Ion Optics. *Review Of Scientific Instruments* **1990,** 61, (10), 2585-2591.
24. Bergmann, T.; Martin, T. P.; Schaber, H., High-Resolution Time-Of-Flight Mass Spectrometers.2. Reflector Design. *Review Of Scientific Instruments* **1990,** 61, (10), 2592-2600.
25. Hydutsky, D. P.; Castleman, A. W.; Bianco, N. J.; Dermota, T., Limited solvation and controlled ion-pair formation in $HX(H_2O)_n$ clusters. *Abstracts Of Papers Of The American Chemical Society* **2005,** 230, U2973-U2973.
26. D. P. Hydutsky, N. J. B., and A. W. Castleman, Jr In *Photodissociation of SO_2 at 200 nm: Evidence of an anisotropy effect*, Femto Chemistry VII Fundamental Processes in Chemistry, Physics, and Biology, Fairmont Washington, Wastington, DC, USA, 2005; Kimble, A. W. C. J. a. M. L., Ed. Elsevier: Fairmont Washington, Wastington, DC, USA, 2005; pp 109-112.
27. Kanamori, H.; Butler, J. E.; Kawaguchi, K.; Yamada, C.; Hirota, E., Spin Polarization In So Photochemically Generated From So2. *Journal Of Chemical Physics* **1985,** 83, (2), 611-615.
28. Parsons, B.; Butler, L. J.; Xie, D. Q.; Guo, H., A combined experimental and theoretical study of resonance emission spectra of SO_2 C $^1B_2$. *Chemical Physics Letters* **2000,** 320, (5-6), 499-506.

Chapter 6

Isotope Effects in the Photodissociation of $^{32}SO_2$, $^{33}SO_2$, an$^{34}SO_2$ at 200 to 197 nm

6.1 Abstract

In an effort to assess the viability of photochemical processes in the Archean era that could have resulted in an unusual sulfur isotope signature in the rock record,[1] pump-probe experiments have been performed on SO_2 at ~200 to 197 nm. We have found several effects: the pump wavelength affects the population of excited species that undergo prompt dissociation, the wavelength of the probe beam also affects the population seen in the experiment, the absorption cross-section of the probe beam is dependent on the isotope of sulfur, and the power of the probe beam affects the populations seen in the experiment. All of these observations are explained in a qualitative fashion by change in rovibrational bands caused by the different sulfur isotopes. The ramification of these isotope effects are discussed with regard to the onset of atmospheric oxygen and the physics that are causing the isotope effects.

6.2 Introduction

The motivation for this work comes from studies of the Earth's history specifically when an oxygen-rich atmosphere, like today's atmosphere, formed. Our collaborators[2] have proposed that the large fluctuations of sulfur isotope abundances seen

in the rock record (Figures 1.2 and 1.3 of Chapter 1) are the result of a photochemical process that fractionated sulfur from SO_2 and eventually deposited it in the Earth's crust. Others[3] have proposed alternate theories on how the unexpected sulfur isotope record arose. These theories are based on the unique chemical composition of the sulfur reducing bacteria of the time. Experiments reported here were performed to determine if photochemical dissociation of SO_2 at 200-197 nm could produce large isotope effects.

6.3 Experimental

The instrument used in these experiments consists of a femtosecond laser system that produces 100 fs pulses, at 10 Hz, with 2.5 mJ per pulse, centered at 800 nm. The fundamental is frequency double and frequency mixed to produce second, third, and fourth harmonics. The second harmonic was used in all cases for the probe beam and the fourth harmonics is used for the pump beam. The system is slightly tunable and specific wavelengths for specific experiments are given in the text. Both pure and mixtures of SO_2 and helium were introduced by a Parker solenoid valve and a pick-up source.[4, 5] No discernable difference between introduction through the solenoid and the pick-up source was seen. We conclude from this and analyses with mass spectrometry that no SO_2 clusters were present in our experiments. Detection of ionized clusters was performed with a home built time-of-flight mass spectrometer consisting of a quadrapole time-of-flight assembly,[6] a reflection,[7] and a Burel bipolar detector. Signal from the detector was acquired by a Tektronics oscilloscope model TDS5104B.

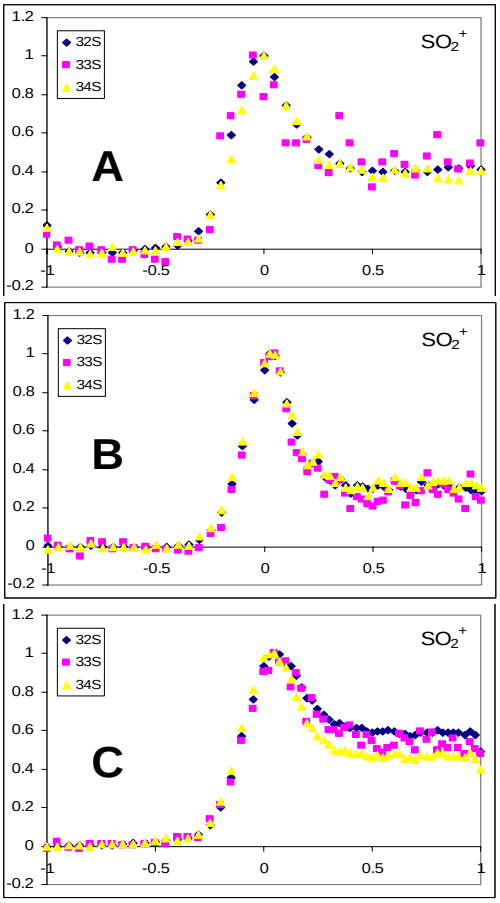

Figure 6.1. Effects of changes in the pump wavelength. A, the pump is at 199.5 nm, B, the pump is at 198.5 nm, and C, the pump is at 197.5 nm.

6.4 Results

Figure 6.1 show three transients at three different pump wavelengths. Note with the pump wavelength at 197.5 nm in **C** of Figure 6.1 an obvious isotope effect can be seen. For either population or absorption cross-section reasons the long decay in the ^{34}S isotope has less amplitude than the ^{33}S and the ^{32}S. As discussed later isotope effects are also seen at longer pump wavelengths but they are not as pronounced and mostly result from wavelength and power effects in the probe beam.

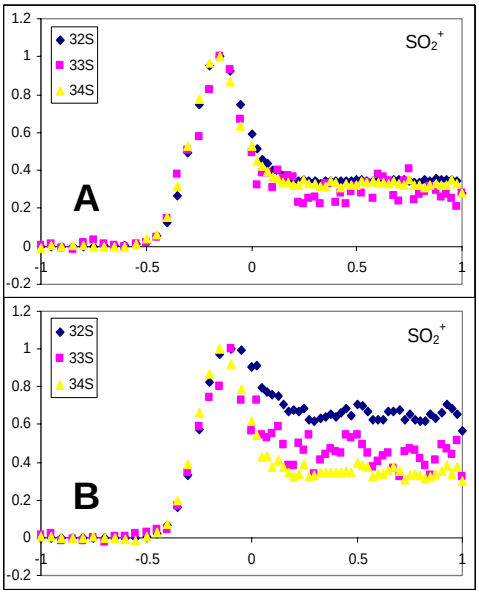

Figure 6.2. Small changes in the probe wavelength can also affect the dynamics. **A,** shows a pump wavelength of 198.5 nm and a probe wavelength of 395.50 nm. **B,** shows the same pump wavelength with a probe of 397.24 nm.

Figure 6.2 shows two transients with the pump wavelength held constant and the wavelength of the probe changed. There is a significant change in the amplitude of the long decay of the various sulfur isotopes upon changing the probe wavelength from 395.5 nm, **A,** to 397.25 nm, **B**. Again, it is not clear whether the changes seen are a result of a different population or a different absorption cross-section for the probe beam.

Figure 6.3 shows the overlay of SO_2 and SO transients of ^{32}S in, **A** and ^{34}S, **B**. These transients are taken from the same pump-probe trace and are identical with respect to power, wavelength, and pressure. One can clearly see that the SO_2 and SO transients in Figure 6.3, **A,** are near perfect overlays of each other, indicating that ion-state fragmentation is dominant. On the other hand Figure 6.3, **B**, shows distinct differences in the SO_2 and SO transients, indicating that a larger amount of the dynamics seen in Figure 6.3, **B**, are actually the neutral state dynamics of the SO fragment (see Chapter 5). This means that the ^{32}S species has a different absorption cross-section for the probe beam

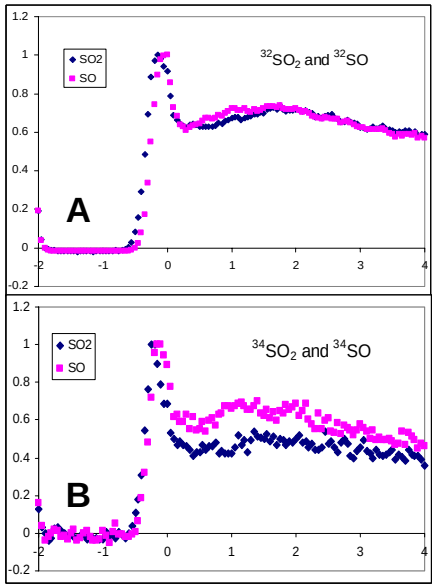

Figure 6.3. The response of SO_2^+ and SO^+ transients for the ^{32}S, A, and ^{34}S isotopes, B. This is the result of different absorption cross section for the probe or differences in population of SO.

than the ^{34}S species at these conditions, or that differences in population are causing the effect.

Figure 6.4 shows the long decay of the $^{32}SO_2$ and $^{34}SO_2$ transient at two different probe powers. In Figure 6.4, **A,** the $^{34}SO_2$ appears to decay more slowly than the $^{32}SO_2$ species, while in at lower power in Figure 6.4, **B**, the two transients overlay nicely. Again this could be due to population or absorption cross-section reasons and as discussed later.

6.5 Discussion

All of the effects that are seen in our experiment must result from either population or absorption cross-section difference. Population arguments could be facilitated if the lifetime of the dissociation was measurable (shorter lifetime implies

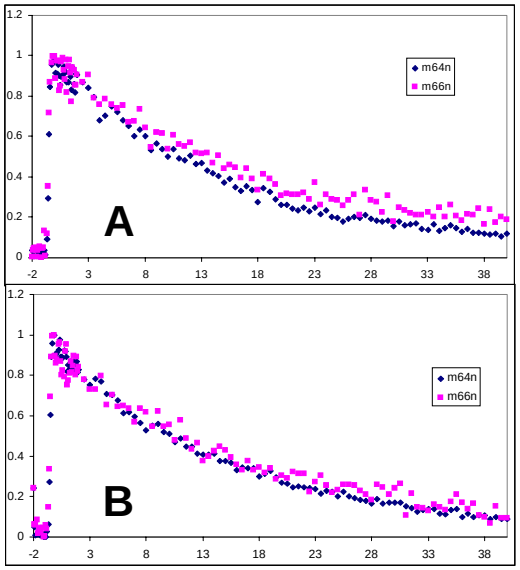

Figure 6.4. The effect of probe power on the SO_2 transients for the ^{32}S and ^{34}S isotopes. **A** shows a transient at probe power 0.19 mJ/pulse while **B** shows a transient where all other variables are the same but the power was dropped to 0.17 mJ/pulse.

more efficient dissociation) but it is not possible under the current setup of our laser (see Chapter 5). Thus we look to the experimental findings for an explanation that does not explicitly require knowledge of either.

The pump wavelength effect can most easily be explained by shifts in the absorption of rovibrational states. If we consider the potential energy surface of SO_2 (see Figure 7 of reference[8]) we see that the excitation region consists of states that are bound and dissociative. The Frank-Condon region of excitation exists in a bound area; to dissociate the excited population must quickly couple to a dissociative state. We can therefore make arguments for asymmetry and density of states, with respect to the bound well, contributing to differences in the rovibrational excited population. As one goes higher in a bound well, the well becomes more asymmetric and wider. These distortions cause the vibrational spacing to decrease and the density of states to increase. A more

massive atom can also cause vibrational spacing to decrease. Thus, we believe that the pump wavelength phenomena observed here can be attributed to differing excited-state rovibrational populations in the isotopes resulting from the asymmetry of the well and the density of states that result.

The probe wavelength and power effects can also be explained from the shifts in vibrational states that we believe are occurring. The existence of these effects is strong evidence for the isotopic sensitivity of SO_2 at these energies. As a visual aid to the reader Figure 6.5 is presented as a conceptual picture of how the probe can have such drastic effects on the signal. Note that in Figure 6.5 all of the vibrational states are spaced evenly and all the populations are the same for a given state and the two isotopes. As we discussed above this is most likely not the case, but this simplistic picture still qualitatively explains the probe phenomena. The first column shows how changes in the probe wavelength can affect the observed signal. Given a set population of in the rovibrational states, changes in the probe wavelength will affect the amount of signal detected for each isotope. The second column shows how changes in the probe power can also affect the amount of signal detected for each isotope. The ionization process is two photons, thus small differences in intensity of the wavelengths in the bandwidth will be squared as per Equation 4.1. As the power is decreased the bandwidth of the probe that is capable of ionizing the SO_2 chromophore shrinks as the ionization process is two photons. As this occurs some of the bands may no longer be effectively ionized, and thus lead to changes in the observed signal.

6.6 Conclusion

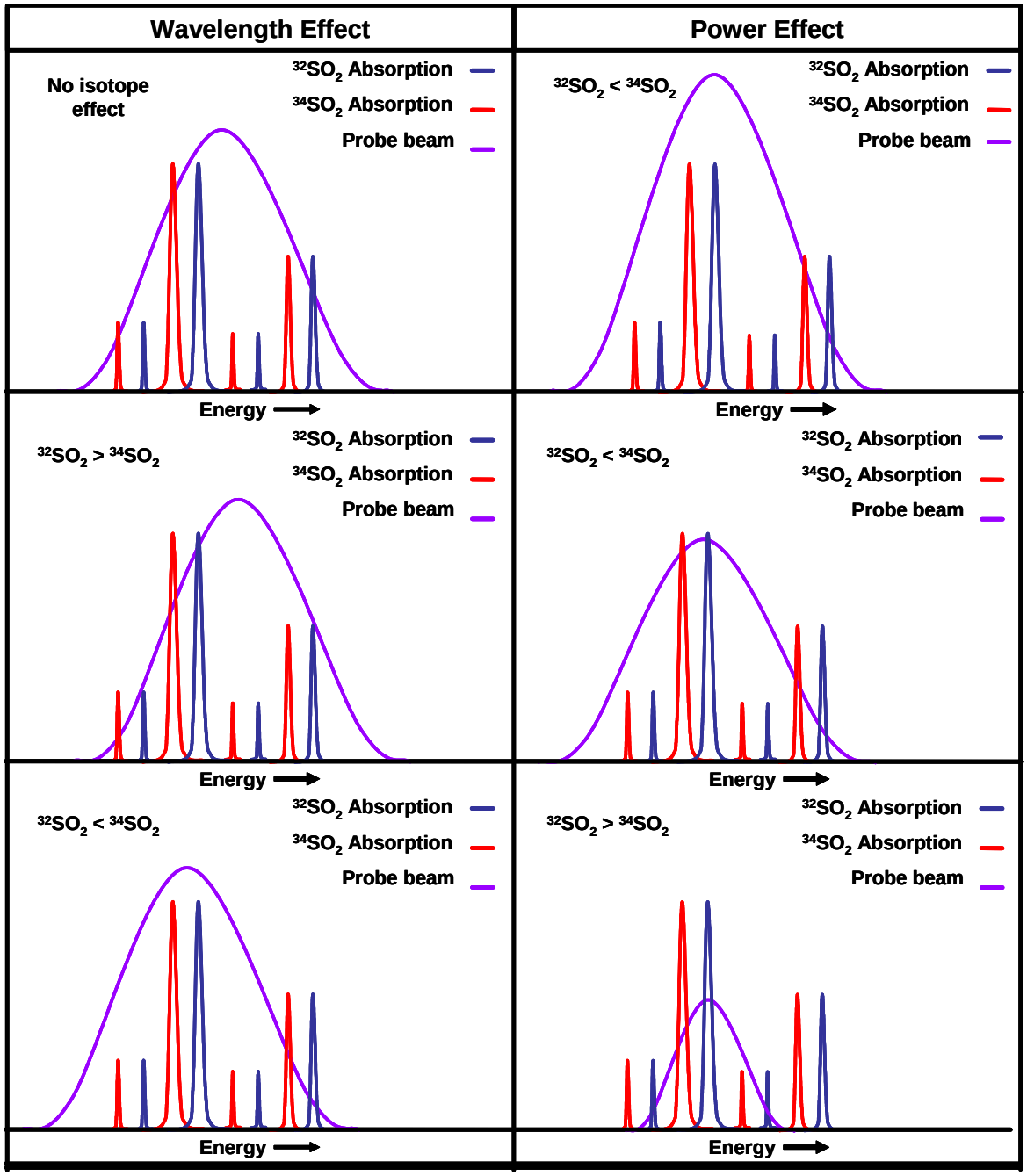

Figure 6.5. This picture is intended as a conceptual aid to help the reader understand how small shifts in the origins of rovibrational states can alter the pump-probe transients. Further explanation is given in the text but in summary a change in the wavelength or power of the probe could cause rovibrational bands from one isotope to be more efficiently ionized then another isotope.

In summary we have observed the following isotope effects: 1) a pump wavelength effect that either causes more efficient dissociation of the heavier sulfur isotopes or results in a smaller absorption cross-section for the probe beam 2) different

isotopes of sulfur have different absorption cross-section for the probe beam depending on the experimental conditions 3) probe wavelength can change the abundance of isotopes detected 4) probe power also affects abundances of isotopes detected. Shifts in the rovibrational states can explain all of the phenomena seen in this experiment. These shifts are most likely not even, and are likely the result of the asymmetry of the bound well in the excitation region combined with the different masses of the sulfur isotopes. There is evidence in the literature for shifts to increase as vibrational levels increase. Studies[9, 10] on the coupled AB state of SO_2 have shown measurable shifts in the origin of vibrational bands of $^{34}SO_2$ from $^{32}SO_2$. These measurements are low in the bound well of SO_2 and show an increase in shift as excitation goes higher into the bound well. The highest shift reported in references 9 and 10 is 9.29 cm^{-1}; our experiments are very high in the bound well where, as mentioned above, anisotropy of the bound well is large and would likely increase the magnitude of the shift. Additionally, Chapter 5 discusses the effects that asymmetric stretches have on the dynamics of SO_2 at these energies. These asymmetric stretches could also influence the behavior of the SO_2 chromophore by breaking the symmetry.

Future experiments will endeavor to explain in greater detail what the physical nature of these isotope effects. By using detection techniques that have less influence on the processes involved, we can determine quantitatively the isotope effects. Photoelectron spectroscopy would be well suited for these experiments because we could examine the influence of the isotopes on the vibrational energies of SO_2. Thus, the shifts proposed here to explain the findings could be measured.

In terms of the astrobiology implications, these experiments show that there are indeed large isotope effects in the photodissociation of SO_2 at these wavelengths. Though we have seen conditions where the lighter isotopes seem to dissociate more efficiently than the heavier isotopes, the general trend is for the heavier isotopes to dissociate more effectively than the lighter isotopes. The difficulties we encountered with ion-state fragmentation and difference absorption cross-section for the probe beam prohibit a quantitative assessment of these findings. Also, our experiments and others[11, 12] show that long lived SO_2 species exist at these excitation energies. This could be important because of other gas phase molecules that could react with or quench the excited SO_2, perhaps leading to more isotope effects.

6.7 References

1. Farquhar, J.; Savarino, J.; Airieau, S.; Thiemens, M. H., Observation of wavelength-sensitive mass-independent sulfur isotope effects during SO_2 photolysis: Implications for the early atmosphere. *Journal Of Geophysical Research-Planets* **2001,** 106, (E12), 32829-32839.
2. Pavlov, A. A.; Kasting, J. F., Mass-independent fractionation of sulfur isotopes in Archean sediments: Strong evidence for an anoxic Archean atmosphere. *Astrobiology* **2002,** 2, (1), 27-41.
3. Ohmoto, H.; Watanabe, Y.; Ikemi, H.; Poulson, S. R.; Taylor, B. E., Sulphur isotope evidence for an oxic Archaean atmosphere. *Nature* **2006,** 442, (7105), 908-911.
4. Goyal, S.; Robinson, G. N.; Schutt, D. L.; Scoles, G., Infrared-Spectroscopy Of SF_6 In And On Argon Clusters In An Extended Range Of Cluster Sizes - Finite-Size Particles Attaining Bulk-Like Properties. *Journal Of Physical Chemistry* **1991,** 95, (11), 4186-4189.
5. Gough, T. E.; Knight, D. G.; Scoles, G., Matrix Spectroscopy In The Gas-Phase - Ir Spectroscopy Of Argon Clusters Containing SF_6 Or CH_3F. *Chemical Physics Letters* **1983,** 97, (2), 155-160.
6. Bergmann, T.; Goehlich, H.; Martin, T. P.; Schaber, H.; Malegiannakis, G., High-Resolution Time-Of-Flight Mass Spectrometers.2. Cross Beam Ion Optics. *Review Of Scientific Instruments* **1990,** 61, (10), 2585-2591.

7. Bergmann, T.; Martin, T. P.; Schaber, H., High-Resolution Time-Of-Flight Mass Spectrometers Part II. Reflector Design. *Review Of Scientific Instruments* **1990,** 61, (10), 2592-2600.
8. Katagiri, H.; Sako, T.; Hishikawa, A.; Yazaki, T.; Onda, K.; Yamanouchi, K.; Yoshino, K., Experimental and theoretical exploration of photodissociation of SO_2 via the C $^1B_2$ state: identification of the dissociation pathway. *Journal Of Molecular Structure* **1997,** 413, 589-614.
9. Huang, C. L.; Chen, I. C.; Merer, A. J.; Ni, C. K.; Kung, A. H., Spectra of jet-cooled $^{32}SO_2$ and $^{34}SO_2$ in systems a^3B_1 and b^3A_2 - X^1A_1: Rotational structure of perturbed b^3A_2. *Journal Of Chemical Physics* **2001,** 114, (3), 1187-1193.
10. Huang, C. L.; Ju, S. S.; Chen, I. C.; Merer, A. J.; Ni, C. K.; Kung, A. H., High-resolution spectroscopy of jet-cooled $^{32}SO_2$ and $^{34}SO_2$: The a^3B_1 - X^1A_1, 2^1_0 and 1^1_0bands. *Journal Of Molecular Spectroscopy* **2000,** 203, (1), 151-157.
11. Parsons, B.; Butler, L. J.; Xie, D. Q.; Guo, H., A combined experimental and theoretical study of resonance emission spectra of SO_2 C^1B_2. *Chemical Physics Letters* **2000,** 320, (5-6), 499-506.
12. Ray, P. C.; Arendt, M. F.; Butler, L. J., Resonance emission spectroscopy of predissociating SO_2 C^1B_2: Coupling with a repulsive $^1A_1$ state near 200 nm. *Journal Of Chemical Physics* **1998,** 109, (13), 5221-5230.

Chapter 7

Conclusion

7.1 Concluding Remarks

The work performed here has helped to elaborate several fundamental processes in chemistry. The work on SO_2 dissociation has shown that under the right circumstances symmetric molecules can produce large isotope effects. The combination of high vibrational excitation, well asymmetry, asymmetric stretching modes, and the proximity to a dissociative state all play important roles in the interpretation of the isotope effects. Excitation high into a bound well, where the asymmetry of the well will decrease the vibrational spacing could result in isotope effects. The higher density of states for the heavier species could lead to the differences in absorption cross-section that we observe and perhaps differences in dissociation efficiencies. These studies show that significant photoinduced isotope effects are possible at these wavelengths and strengthen the hypothesis that the sulfur isotope fluctuations in the rock record could be caused by a photochemical route. Further studies with faster laser pulses and a less invasive detection technique could quantify these effects.

Our studies of $HI(H_2O)_n$ clusters have revealed strong evidence for the theoretically proposed biradical species and thus question cavity models of the solvated electron. While the body of work that exists is not sufficient to eliminate the cavity model, it does justify alternative interpretations and open up the field for more studies so

that a model that satisfies all the experimentally measured phenomena can be found. Our experiments also provide support of theoretical prediction of ground-state ion-pair formation in $HI(H_2O)_n$ clusters. This, along with our previous work on $HBr(H_2O)_n$ and $HI(H_2O)_n$ clusters, provides firm benchmarks for high-level computational chemistry. The continuation of this work into systems like $NaI(H_2O)_n$ would assess the atmospheric viability of the mechanism studied in this work. From the known ionization potentials of NaI, the wavelengths necessary to form biradicals in sea-salt aerosols would be in an atmospherically relevant range; thus biradical formation could influence halogen removal in low water sea-salt aerosols.

Vita

Darren P. Hydutsky

Education

Ph.D., Physical Chemistry, Penn State University, University Park, PA, May 2007
B.S. in Chemistry, Millersville University, Millersville, PA, 2000
B.S. in Mathematics, Millersville University, Millersville, PA, 2000

Experience

Research

Summer of 2001 to present – Research assistant to Dr. A. W. Castleman, Jr., Penn State University

Teaching

Fall of 2000 – Teaching assistant for general chemistry laboratory, Penn State University
Spring of 2001 – Teaching assistant for general chemistry laboratory, Penn State University

Industrial

Summer of 1999 – RECRA Environmental Laboratory, Digestion Technician, Eagle, PA

Presentations

"Limited solvation and controlled ion-pair formation in $HX(H_2O)_n$ clusters"
D. P. Hydutsky, A. W. Castleman, Jr., N. J. Bianco, and T. E. Dermota
Talk presented at ACS National Conference, September **2005**, Washington DC.

"Dissolution of Simple Systems: Acid Halides and Water."
D. P. Hydutsky, A. W. Castleman, Jr., and N. J. Bianco
Talk presented at Telluride Solvation Conference, August **2006**, Telluride, CO.

Selected Publications

"Photo-Induced Ion-Pair Formation in the $(HI)_m(H_2O)_n$ Cluster System" T. E. Dermota, D. P. Hydutsky, N. J. Bianco, and A. W. Castleman, Jr., Journal of Chemical Physics, Vol. 123, article number 214308, **2005**.

"Photodissociation of SO_2 at 200 nm: Evidence of an anisotropy effect"
D. P. Hydutsky, N. J. B., and A. W. Castleman, Jr., Femtochemistry VII Fundamental Processes in Chemistry, Physics, and Biology, Edited by: M. L. Kimble and A. W. Castleman, Jr., Elsevier, Fairmont Washington, Washington, DC, USA, **2005**; pp 109-112.